K/SUB/93-XJ947/2R1

K-25

OAK RIDGE
K-25 SITE

LOCKHEED MARTIN

HGSYSTEM/UF_6 MODEL ENHANCEMENTS FOR PLUME RISE AND DISPERSION AROUND BUILDINGS, LIFT-OFF OF BUOYANT PLUMES, AND ROBUSTNESS OF NUMERICAL SOLVER

Steven R. Hanna
Joseph C. Chang
EARTH TECH, Inc.
196 Baker Avenue
Concord, MA 10742

January 1997

MANAGED BY
LOCKHEED MARTIN ENERGY SYSTEMS, INC.
FOR THE UNITED STATES
DEPARTMENT OF ENERGY

UCN-13671 (16 6-95)

K/SUB/93-XJ947/2R1

Gaseous Diffusion Plant
Safety Analysis Report Upgrade Program

HGSYSTEM/UF_6 MODEL ENHANCEMENTS FOR PLUME RISE AND DISPERSION AROUND BUILDINGS, LIFT-OFF OF BUOYANT PLUMES, AND ROBUSTNESS OF NUMERICAL SOLVER

January 1997

Document authored by
Steven R. Hanna
Joseph C. Chang
EARTH TECH, Inc.
196 Baker Avenue
Concord, MA 10742
under Subcontract No. 1AK-XJ947C
with
LOCKHEED MARTIN ENERGY SYSTEMS, INC.
managing the
Oak Ridge K-25 Site
and
Oak Ridge Y-12 Plant
and the
Environmental Management Activities
Paducah Gaseous Diffusion Plant
Portsmouth Gaseous Diffusion Plant
for the
U.S. DEPARTMENT OF ENERGY
under contract DE-AC05-84OR21400

CONTENTS

FIGURES

ACRONYMS

ASHRAE	American Society of Heating, Refrigerating and Air-Conditioning Engineers
EPA	Environmental Protection Agency
ftp	file transfer protocol
GDPs	gaseous diffusion plants
ISC	Industrial Source Complex
LMES	Lockheed Martin Energy Systems, Inc.
NAG	Numerical Algorithms Group
SAR	Safety Analysis Report
SLATEC	Sandia, Los Alamos, Air Force Weapons Laboratory Technical Exchange Committee

1. BACKGROUND AND OBJECTIVES

The HGSYSTEM/UF_6 model was developed for use in preparing Safety Analysis Reports (SARs) by estimating the consequences of possible accidental releases of UF_6 to the atmosphere at the gaseous diffusion plants (GDPs) located in Portsmouth, Ohio, and Paducah, Kentucky (Hanna et al. 1996). Although the latter report carries a 1996 date, the work that is described was completed in late 1994. When that report was written, the primary release scenarios of interest were thought to be gas pipeline and liquid tank ruptures over open terrain away from the influence of buildings. However, upon further analysis of possible release scenarios, the developers of the SARs decided it was necessary to also consider accidental releases within buildings. Consequently, during the fall and winter of 1995–96, modules were added to HGSYSTEM/UF_6 to account for flow and dispersion around buildings.

The original HGSYSTEM/UF_6 model also contained a preliminary method for accounting for the possible lift-off of ground-based buoyant plumes. An improved model and a new set of wind tunnel data for buoyant plumes trapped in building recirculation cavities have become available that appear to be useful for revising the lift-off algorithm and modifying it for use in recirculation cavities (Briggs, 1996). This improved lift-off model has been incorporated in the updated modules for dispersion around buildings.

In the spring and summer of 1995, EARTH TECH and Lockheed Martin Energy Systems, Inc. (LMES) engineers performed extensive testing of the aerosol jet (AEROPLUME/UF_6) algorithm in HGSYSTEM/UF_6. These tests revealed that the model runs occasionally failed, primarily during scenarios in which the modeled dense UF_6 plume sank towards the ground and was deflected horizontally after striking the ground. A major part of this problem was identified as the numerical solution procedure implemented by the code at that point. Plans were therefore made for revising the solution methodology so it would be more robust and the model would run successfully for a wider range of release scenarios.

This report contains technical documentation and a user's guide (see Appendix A) for the following revised components of HGSYSTEM/UF_6:

- A plume trajectory, dispersion, and lift-off model has been added for warm plumes released from roof vents and exhaust ducts on large process buildings at GDPs.

- A plume trajectory, dispersion, and lift-off model has been added for UF_6 plumes released from open bay doors on transfer buildings at GDPs.

- A more dependable solution methodology for AEROPLUME/UF_6 has been implemented.

The materials in this report are intended to complement the original HGSYSTEM/UF_6 report (Hanna et al., 1996). The reader should have that report available for reference to better understand the technical documentation in this report and to be able to follow the user's guide included in Appendix A.

2. CHARACTERISTICS OF SOURCE SCENARIOS FOR ACCIDENTAL UF_6 RELEASES FROM PROCESS AND TRANSFER BUILDINGS AT GDPs

Two source scenarios for accidental UF_6 releases have been considered in order to make modifications to HGSYSTEM/UF_6. In the first scenario, the UF_6 is assumed to be released from a ruptured gas pipeline inside a large process building at a GDP, where the UF_6 completely reacts with water vapor inside the building; thus, a warm plume of UO_2F_2 and $HF{\cdot}H_2O$ products is emitted into the ambient atmosphere through forced-air roof vents and motor exhaust ducts. In the second scenario, the UF_6 is assumed to be released from a break of a liquid line in a transfer building at a GDP, where the UF_6 may not completely react with water vapor inside the building, and enters the ambient atmosphere through open bay doors on the side of the building. These scenarios are described in more detail below; the specific building dimensions and information on vent sizes and air speeds are provided in October 10, 1995, and November 3, 1995, memos from Russell W. Schmidt (1995) of LMES.

2.1 Release from Roof Vent or Motor Exhaust Duct on a Process Building at a GDP

The seven process buildings at the Paducah and Portsmouth GDPs are low and flat, with heights ranging from 18.9 to 25.3 m and areas ranging from about 4.7×10^4 m^2 to about 1.3×10^5 m^2 (i.e., the side dimensions are about 170 to 300 m by about 250 to 650 m). The building widths, W_B, are therefore about 10 to 20 times the building heights, H_B. Each building contains 4 to 8 process units and each unit has 10 roof vents and 2.5 (in some cases, 2 units share 5 exhaust ducts) to 4 motor exhaust ducts. The roof vents are uniformly spaced about 30 to 40 m apart on the roof of the process building. The motor exhaust ducts are all located on the edges of the roof, with spacings of about 50 to 100 m apart. The flow from all vents and ducts is driven at a constant rate at all times by a fan.

It is assumed that an accidental release is associated with a rupture occurring on one of the pipelines (with about 0.5 m diam) carrying warm UF_6 gas in the process building. Only one process unit is assumed to be affected. The UF_6 gas is released in the building where it reacts with ambient water vapor. It is further assumed that there is sufficient water vapor in the building so that all reactions take place inside the building. The reaction products, UO_2F_2 and $HF{\cdot}H_2O$, are therefore assumed to be emitted as passive (i.e., nonreactive) materials from the roof vents and motor exhaust ducts.

The time duration of the release from the process building is on the order of 1 hour, thus allowing the dispersion process to be simulated as a continuous plume for averaging times up to 1 hour. Due to the heat constantly generated by normal operations of the gaseous diffusion process, the mixture coming out of the vents and ducts is at least 20 to 30 K above the outside air temperature. The heat generated inside the building by chemical reactions during an accidental release may further increase the plume temperature.

The roof vents each have a volume flow rate of about 20.8 m^3/s, a fan-driven velocity of 7 m/s, and an area of 3 m^2. However, each vent has a roof cap (to keep out precipitation), which causes the initial momentum jet to be deflected sideways. The motor exhaust ducts on the outside edges of the process buildings each have a volume flow rate of 89.2 m^3/s, a fan-driven velocity of 4.3 m/s, and an area of 20.7 m^2. They are not capped. The roof vents and motor exhaust ducts are flush with the top of the process building.

An alternate scenario involves the removal of the motor exhaust ducts in an earthquake. In this case, the warm air would no longer be vented upward but would be vented horizontally through an opening that is halfway up the side of the building, at a height of about 10 m. The area of that opening is 8.1 m^2. Assuming a volume flow rate 89.2 m^3/s, the horizontal release velocity is about 11 m/s.

2.2 Release from Open Doors on a Transfer Building at a GDP

The second primary source release scenario of interest in this report concerns the accidental rupture of a valve or pipe when liquid UF_6 is being transferred from one container to another. These transfer operations take place at the GDPs inside a transfer building of height 11 to 14 m, width 24 to 46 m, and length 47 to 122 m. The release would occur inside the building at a position 10 or 20 m from the end of the building. Bay doors are assumed to be opened so that part of the side area of that end of the building is open to the outside. The liquid jet of UF_6, with assumed mass emission rate of 1 to 10 kg/s, could be released at any angle inside the building. The resulting plume is mixed with air inside the building as it passes over and around several obstructions (e.g., tanks, pipe racks) before exiting through the doors. The maximum possible cross-sectional area of the plume is obviously the area of the door opening. A fraction, f_A, is defined to be the ratio of the plume cross-sectional area as it exits the building to the area of the end of the building. This ratio has been assumed to vary from about 0.001 to 1.0 at various transfer buildings. Unfortunately, it is only possible to approximately estimate f_A because this parameter depends on many uncertain factors, such as the geometrical configuration of pipes and tanks in the building. The assumption is made that the plume is diluted in a volume flow rate given by the product of the factor f_A times the area of the end of the building, A_B, times the ambient wind speed, $u_{H/2}$, at a height of ½ the building height.

All reactions cannot be assumed to have taken place before the plume enters the ambient atmosphere. As mentioned in the previous paragraph, the volume flow rate of the plume at the point it passes through the bay doors is assumed to equal $u_{H/2} \cdot f_A \cdot A_B$. Given this plume volume flow rate, the concentrations of UF_6 gas, the UF_6 solid, UO_2F_2, and $HF \cdot H_2O$ in the plume must be calculated downwind of the transfer building.

The time duration of the release, T_d, from the transfer building is expected to be a few minutes. Consequently, predicted concentrations will vary with time.

3. PLUME RISE ESTIMATES FOR MOTOR EXHAUST DUCTS AND ROOF VENTS ON PROCESS BUILDINGS AT GDPs

On October 10, and November 3, 1995, R. W. Schmidt (1995) of LMES distributed memos containing information on the flow from the motor exhaust ducts and roof vents on the Portsmouth and Paducah GDP process buildings. Dimensions of the buildings are also given and discussed in Sect. 2. For example, the building heights range from about 19 to 25 m, and the building widths range from 170 to 650 m.

The purpose of this section is to apply some standard analytical plume rise formulas to determine the typical range of plume rise from the ducts and vents and to compare these estimates with the expected height of the recirculation cavity. This is important because if the plume rise is relatively small, the plume may be caught and mixed in the recirculation cavity next to the ground. Conversely, if the plume rise is relatively large, the plume will be above the recirculation cavity and can be modeled with a standard Environmental Protection Agency (EPA) model such as Industrial Source Complex (ISC) Version 3 (EPA, 1995).

The flow rates from the ducts and vents given by Schmidt were converted to the standard dimensional forms required by Briggs' (1975; 1984) plume rise equations, as given below:

Volume Flux, V_o = 89.67 m^3/s for ducts and 20.77 m^3/s for vents,

Plume Speed, w_o = 4.3 m/s for ducts and 7.0 m/s for vents,

Momentum Flux, $M_o = w_o \frac{V_o}{\pi}$ = 123 m^4/s^2 for ducts and 46.3 m^4/s^2 for vents, and

Buoyancy Flux, $F_o = \frac{g}{T} \Delta T \frac{V_o}{\pi}$ = 28.5 m^4/s^3 for ducts and 6.6 m^4/s^3 for vents,

where g is the acceleration of gravity (9.8 m/s^2), T is the absolute temperature (K) of the plume (assumed to be equal to 330 K in these calculations), and ΔT is the difference between the plume and ambient air temperature (K). These estimates are based on ΔT ~30 K (Goode and Schmidt, 1995) and w_o calculations made by Schmidt (1995). In calculating plume rise from the capped vents, the buoyancy flux will be considered, but momentum flux will be ignored (ASHRAE, 1993). The caps are assumed to dissipate the initial vertical momentum. It should be noted that the temperature difference, ΔT, may vary in time due to chemical and thermodynamics effects, which will tend to increase the temperature of the plume. The assumption of ΔT ~30K leads to conservative (i.e., lower) estimates of plume rise.

The motor exhaust ducts are located around the edges of the building, with spacing of 50 to 100 m. The vents are uniformly spaced over the roof and are separated by about 30 to 40 m. Any wind direction is possible.

Some scaling comparisons can be made by using the above estimates. First, note that for the process buildings described by Schmidt (1995), there are 40 to 110 vents and 10 to 32 ducts per building. The total maximum buoyancy flux from the vents and ducts on the largest process building is about 1400 m^4/s^3, or about 160 MW. The total maximum volume flux from the vents and ducts on the largest process building is about 4700 m^3/s, which can be compared with the volume flux of air impacting the upwind process building face:

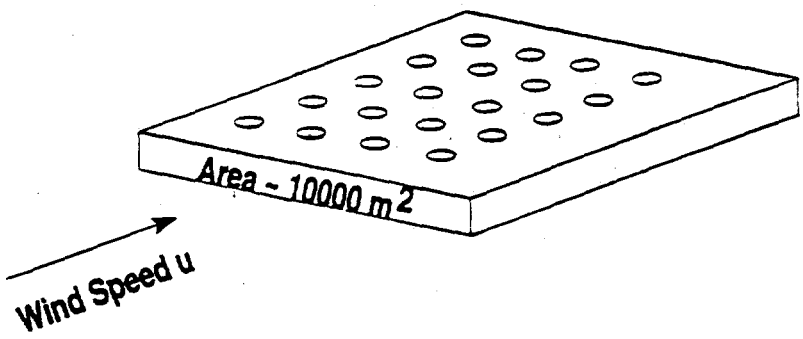

$$\text{Fraction} = \frac{\text{volume flux from vents and ducts}}{\text{ambient volume flux}} = \frac{4700\ m^3/s}{u \cdot 10000\ m^2} .$$

This "fraction" equals 0.47, 0.23, 0.09, and 0.05 for wind speeds, u, of 1, 2, 5, and 10 m/s, respectively. It can be concluded that, for low wind speeds, the volume fluxes from the vents and ducts may be large enough to generate a circulation pattern over the process building. The small diagram below illustrates the types of circulations likely to be observed.

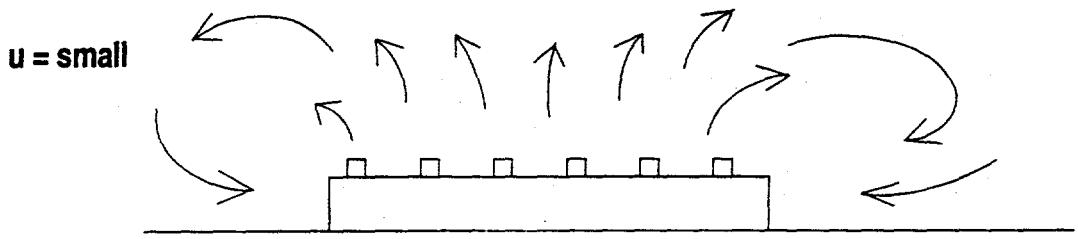

The gradual plume rise in the first few tens of meters downwind of a single duct can be estimated from the formula (Briggs, 1984)

$$\Delta z = \left(19 \frac{M_o}{u^2} x + 4.2 \frac{F_o}{u^3} x^2 \right)^{1/3} , \quad (1)$$

where Δz is the elevation of the plume centerline above the source elevation, and x is downwind distance. It is of interest to determine the plume rise at the downwind edge of the cavity or wake, where x is equal to 4 or 5 building heights, or about 100 m (Hosker, 1984). If the plume rise at the end of the wake is greater than 1.5 building heights (about 38 m in this case), it is EPA's (1995) procedure to assume that the plume is unaffected by the wake. Assuming that $F_o \approx 29$ m^4/s^3 and $M_o \approx 123$ m^4/s^2 for an individual exhaust duct, the following plume rise, Δz (at $x = 100$ m), from a duct can be calculated from Eq. (1).

u (m/s)	Eq. (1) Momentum Term (m^3)	Eq. (1) Buoyancy Term (m^3)	Δz Plume rise from ducts (at $x = 100$ m)
1	2.3×10^5	1.2×10^6	113 m
2	5.8×10^4	1.5×10^5	59 m
5	9.3×10^3	9.7×10^3	27 m
10	2.3×10^3	1.2×10^3	15 m

Similar calculations show that Δz at $x = 100$ m for the roof vents is about 60 to 70% of the Δz for the motor exhaust ducts for buoyancy-dominated conditions. It is seen in the table above that, for the ducts, the momentum term dominates the buoyancy term for wind speeds higher than about 5 m/s. The values for Δz, above stack top at $x = 100$ m, are 59 m or greater for light winds ($u \leq 2$ m/s) and 27 m or less for high winds ($u \geq 5$ m/s). This plume rise estimate is therefore greater than 1.5 building heights (38 m) for wind speeds less than 5 m/s. In these cases the plume is therefore unlikely to "downwash" into the building wake.

A major conclusion of this plume rise analysis is that, for typical motor exhaust ducts on GDP process buildings, the plume is likely to rise out of the area influenced by the building wake for wind speeds less than 4 m/s. The plume may be at least partially influenced by the wake at wind speeds higher than 5 m/s.

For the roof vents on the GDP process buildings, where the momentum term can be discounted because of the cap on the vent (ASHRAE, 1993), and where the buoyancy flux is a factor of four less than that for the motor exhaust ducts, the critical wind speed for wake interaction would drop by about a factor of two. In other words, the plumes from the roof vents may interact with the process building wake for $u \geq 2$ to 5 m/s, whereas the plumes from the motor exhaust ducts may interact with the process building wake for $u \geq 5$ to 10 m/s.

Equation (1) is used to calculate the gradual plume rise, Δz, near the source. However, at a downwind distance of 200 to 400 m, the plume reaches final plume rise, Δh, which can be calculated at the GDP process buildings from the following standard formulas:

Momentum final plume rise

$$\Delta h_{mom} = 4.8 \frac{M_o^{1/2}}{u} \quad . \tag{2}$$

Buoyant final plume rise (unstable or neutral ambient conditions)

$$\Delta h_{buoy} \text{ (neutral)} = 21.4 \frac{F_o^{3/4}}{u} \quad . \tag{3}$$

Buoyant final plume rise (stable ambient conditions)

$$\Delta h_{buoy} \text{ (stable)} = 2.6 \left(\frac{F_o}{uS} \right)^{1/3} \quad , \tag{4}$$

where $S = \frac{g}{T} \frac{\partial \theta}{\partial z}$ is ambient stability, which can be assumed to equal 0.00065 s^{-2} for stability class E, and 0.0011 s^{-2} for stability class F. The values are based on gradients ($\partial\theta/\partial z$) of 0.02 and 0.035°C/m for stability classes E and F, respectively, which are the default values assumed by the EPA's ISC3 model (EPA, 1995).

These formulas can be applied to give the final plume rise predictions listed below for the motor exhaust ducts and the roof vents.

Final Plume Rise

u (m/s)	Eq. (2) Δh_{mom} (m)		Eq. (3) Δh_{buoy} (neutral) (m)		Eq. (4) Δh_{buoy} (stable, class F) (m)	
	duct	vent	duct	vent	duct	vent
1	53	0	267	92	77	48
2	27	0	134	46	61	38
5	11	0	53	18	45	28
10	5.3	0	27	9.2	36	22

The final rise from the motor exhaust ducts on the process buildings is seen to be larger than 30 m (1.5 times the process building height) for most Δh_{buoy} predictions in the above table. However, as suggested by the EPA (1995), this final rise occurs at $x = 49\ F_o^{5/8}$, or 400 m, which is 300 m downwind of the building recirculation cavity. For this reason, the "gradual rise" Eq. (1) is more appropriate for determining whether the plume from the motor exhaust ducts interacts with the process building wakes at the GDPs.

As far as the roof vents are concerned, the above table shows that the final buoyant plume rise is larger than 1.5 times the building height only for wind speeds less than 2 m/s during neutral and stable conditions. This final plume rise occurs at a downwind distance of 160 m, or 60 m beyond the end of the process building recirculation cavity. However, because the conservative assumption has been made that $\Delta T \sim 30$ K, these final plume rise estimates are all lower than they would be if the effects of heat additions due to chemical reactions were accounted for.

The question also arises whether the plumes from adjacent vents or ducts on the process building will interact with each other as they rise. If the plumes interact, the combined plume will rise higher than the individual plumes. Briggs (1975) suggests that this interaction will occur only if the final plume rise is much greater than the distance separating the sources. Because the above plume rise calculations show that the final plume rise from the roof vents is usually less than the 30 or 40 m separating them, and the final plume rise from the ducts is usually less than the 50 to 100 m separating them, it is assumed that there are no interactions among neighboring plumes as they rise. It is noted that interactions are likely to occur only during relatively light wind speeds, when final plume rise is relatively large and ground-level concentrations would be relatively low.

4. REVISED MODELS FOR DISPERSION AND LIFT-OFF IN AND DOWNWIND OF THE RECIRCULATION CAVITY OF GDP PROCESS BUILDINGS

The coding for the original HGSYSTEM/UF_6 model described by Hanna et al. (1996) was completed in late 1994. A stand-alone module was included for estimating the concentrations of passive gases on building roofs and sides due to low-momentum releases from flush vents on buildings. This very conservative model was based on a standard model developed by Wilson and Britter (1982) using wind tunnel observations. Because the model is most valid for plumes with small momentum and buoyancy fluxes that exhibit little or no plume rise, it is likely to overpredict concentrations resulting from the buoyant plumes associated with the roof vents and motor exhaust ducts on the GDP process buildings described in Sects. 2 and 3. This overprediction is because the plumes from these vents and ducts have enough buoyancy to cause them to rise 20 or 30 m or more above the building roof. It was decided to revise the algorithms in HGSYSTEM/UF_6 based on updates to roof vent models by Wilson (1995) that better account for the effects of plume buoyancy.

The version of HGSYSTEM/UF_6 completed in late 1994 and described by Hanna et al. (1996) contains a lift-off algorithm based on a preliminary analysis by Briggs (1973). This method is implemented within the AEROPLUME and HEGADAS modules. However, Briggs (1996) recently updated his model to reflect more recent comprehensive wind tunnel observations by Hall and Waters (1986) and Hall et al. (1995) of lift-off of buoyant plumes released into building wakes. It is appropriate to also update HGSYSTEM/UF_6 to reflect the revised lift-off model.

This section presents the derivations, the rationale, and the results of some test cases for the new models for dispersion in, and downwind of, the wake of process buildings. The revised models also incorporate the physical principals in Briggs' (1996) recent lift-off model. As will be seen, it is assumed that all UF_6 reactions are complete in the process building scenario, which allows the plume to be treated as a buoyant plume with conservation of plume materials (UO_2F_2 and $HF{\cdot}H_2O$). Section 5 will discuss the transfer building scenario, where the model must account for the possibility of chemical reactions and varying plume buoyancy flux after the plume leaves the building.

4.1 Assumptions for Source Terms for GDP Process Buildings

The location, dimensions, volume fluxes, momentum fluxes, and buoyancy fluxes for the plumes emitted from the roof vents and motor exhaust ducts (either in place or removed) on the GDP process buildings are described in Sect. 2.1 and Sect. 3. The preliminary calculations of plume rise in Sect. 3, which assumed a temperature difference of 30 K, show that the plumes were sufficiently buoyant to rise far enough to avoid the building recirculation cavity for wind speeds less than 4 or 5 m/s. These calculations also show that interactions between neighboring rising plumes occur only during relatively light wind speeds, when final plume rise is large. If the buoyancy flux were to increase, due to the heat generated by chemical reactions inside the building, the plume rise would increase and the ground-level concentrations would decrease.

It is assumed that all reactions have taken place inside the process building and, hence, that the reaction products (UO_2F_2, $HF{\cdot}H_2O$) are dispersed outside of the building as nonreactive gases. Consequently all dispersion modeling for the process building scenario can be carried out in terms of the scaled concentrations C/Q, where C is the concentration (g/m^3) and Q is the mass emission rate (g/s). Given predictions of C/Q from the model, the dimensional concentration can be obtained by multiplying by Q, which can be assumed to be constant in time for each chemical compound. The contributions to the total concentration at a given receptor from several individual vents or ducts can then simply be added to give the final prediction.

In many cases, the plume temperature and velocity can be assumed to be unaffected by the thermodynamic changes caused by chemical reactions and phase changes within the building. However, if the plume characteristics are slowly varying with time due to chemical reactions and thermodynamic effects, the code can be run in a piecewise fashion; that is, assuming the release is composed of many time segments, where the plume conditions are assumed constant for each time segment. The final results can then be obtained by using the method of superposition, which is not done by the code, but must be done by the user.

The revised model has been developed primarily for the plume types and building shapes that are characteristic of the GDP process buildings. But because the formulations are based on wind tunnel studies involving many types of buildings and plumes, they can be applied to a broad range of plumes emitted from industrial buildings.

4.2 Shape and Dimensions of a GDP Process Building Recirculation Cavity

Downwind of a building, a turbulent recirculation cavity (closely related to the building wake) exists that strongly influences plumes that are located in or near the recirculation cavity (Hosker, 1984). It is important to define the shape of the recirculation cavity that is present downwind of the GDP process buildings. Schulman and Scire (1993) review this subject and suggest the following formula for the length, L_R, of the recirculation cavity for buildings whose length exceeds three times their height:

$$\frac{L_R}{H_B} = \frac{1.3\ (W_B/H_B)}{(1\ +\ 0.25(W_B/H_B))}\ , \qquad (5)$$

where H_B is building height and W_B is building width. The constant, 0.25, is taken from Hosker (1984). Since the ratio W_B/H_B is about 10 or 20 for the GDP process buildings, it is expected that L_R equals $4H_B$, or 80 to 100 m. Schulman and Scire (1993) recommend that, for long buildings, the height of the recirculation cavity, H_R, can be assumed to equal the building height, H_B. Furthermore, for wide buildings, the width of the recirculation cavity, W_R, can be assumed to equal the building width, W_B. Therefore, a picture of the recirculation cavity emerges in which its length is $4H_B$, its height is H_B, and its width is W_B

4.3 Concentration Formulas for Part of a Plume In the Recirculation Cavity of a GDP Process Building

Following the procedures recommended by ASHRAE (1993), Schulman and Scire (1993), and Wilson (1995), it is assumed that a fraction, f_c, of the elevated plume from the ducts or vents is captured by the recirculation cavity and that the remaining fraction, $1-f_c$, of the elevated plume escapes the cavity. The fraction f_c is determined by calculating the plume rise at a distance equal to the end of the recirculation cavity, L_R, using Eq. (1). The distance to the end of the cavity is $x_b + L_R$ for the roof vents and motor exhaust ducts, where x_b is the downwind distance from the roof vent or motor exhaust duct to the downwind edge of the building. Note that the momentum flux, M_o, should be assumed to be zero for the capped roof vents or for the motor exhaust duct scenario where the duct structure is removed by an earthquake. Assuming that the plume rises such that its centerline height equals h_c and that the vertical distribution of concentration in the plume at the end of the recirculation cavity is Gaussian with standard deviation σ_z, then f_c is given by the formula

$$f_c = 0.5\left(1 + erf\left(\frac{H_B - h_c}{\sqrt{2\sigma_z}}\right)\right) \quad , \tag{6}$$

where *erf* is the error function. The centerline height, h_c, is given by H_B plus the plume rise, Δz, for the standard roof vents and motor exhaust ducts, and given by $H_B/2$ plus the plume rise, Δz, for the scenario where the duct structure is removed by an earthquake. The vertical standard deviation, σ_z, at the end of the cavity (i.e., at a distance of $x_b + L_R$ from the source vent) is assumed to be given by the formula proposed by Wilson and Britter (1982) for nonbuoyant plumes from roof vents:

$$\sigma_z = 0.21\ R^{0.25}\ x^{0.75} \quad , \tag{7}$$

where R is the scaling length for the building, defined by

$$R = H_B^{2/3}\ W_B^{1/3} \quad , \tag{8}$$

with the restriction that W_B is set equal to $8H_B$ if $W_B/H_B > 8$.

The source term for the part of the plume trapped in the recirculation cavity is assumed to equal the fraction, f_c, times the total initial source strength:

$$Q_c = f_c\, Q \qquad \text{(for plume trapped in cavity).} \tag{9}$$

For the part of the plume trapped in the recirculation cavity, and at small distances from the source, the concentrations on the building or in the recirculation cavity at the ground along the plume

centerline are given by a formula suggested by Wilson (1995) in his recent updated document prepared for ASHRAE:

$$C_c = \frac{Q_c}{V_o \left[1 + 13 \left(\frac{T_a}{T_s} \right)^{1/2} \frac{w_o}{u_H} \right] + \frac{u_H x_s^2}{16}} , \qquad (10)$$

where V_o is the initial volume flux from the vent, w_o is the initial plume speed, T_a and T_s are air and initial plume temperature (K), u_H is wind speed at building top, and x_s is the "stretched string" distance from the source (the vent opening) to the receptor. Note that the distance, x_s, should account for vertical separations as well as horizontal separations between the source and the receptor. The first V_o term is included in Eq. (10) to make sure that the predicted concentrations do not exceed the initial concentration, $C_0 = Q_c/V_o$, in the vent plume. The second term (with T_a/T_s) accounts for reductions in concentrations due to the initial rise of the momentum jet [this term should be set equal to zero for capped roof vents according to ASHRAE (1993)]. The third term, involving $u_H x_s^2/16$, accounts for plume dilution with increasing downwind distance, x_s, and is similar to the vent plume algorithm already in HGSYSTEM/UF_6, which is valid for zero momentum vents.

It is assumed that the Wilson (1995) model [Eq. (10)] applies at small distances in the building recirculation cavity until the plume grows such that the predicted concentrations drop to the concentrations predicted by a model for a well-mixed recirculation cavity (ignoring buoyant plume lift-off for the time being). The well-mixed cavity model that is proposed was suggested by Briggs (1996) for warm plumes emitted uniformly from a building face. Briggs' empirical formula was obtained by plotting wind tunnel data from Hall and Waters (1986) and Hall et al. (1995) in dimensionless form, as $C_c u_H R^2/Q_c$ versus $F_{**} = F_o/u_H^3 W_B$ for three values of x/H_B (1.2, 12, and 40). Note that in this analysis, x is defined as the distance from the downwind edge of the building. Also, in the experiments and in Briggs' analysis, the plume is completely entrained in the recirculation cavity ($f_c = 1.0$). The wind speed, u_H, is the value at a height of H_B. The concentration, C_c, is always the value at ground level. F_{**} values of about 0.0001, 0.0003, 0.001, 0.003, 0.01, 0.03, 0.1, and 0.3 were tested in the Hall and Waters (1986) wind tunnel experiments, which involved building geometries where the building width was twice the building height. Wind directions perpendicular to the building were emphasized, although some tests with off-angles were also included. The later set of wind tunnel experiments (Hall et al., 1995) involved more complicated release from a variety of vent configurations, building shapes, and wind angles. The empirical formula given below provides a conservative best-fit to the wind tunnel data. It has been derived in 1995 and 1996 as a result of collaborations between the authors and G. A. Briggs. Briggs' (1995) original formula was tested and modified by the authors, who proposed an alternate formula, which was then further modified by Briggs (1996) to give the following result:

$$\frac{CuR^2}{Q} = \frac{\exp(-6F_{**}^{0.4})}{\left[0.037 + 0.03 \left(\frac{x}{H_B} \right)^2 + F_{**}^2 \left(\frac{x}{H_B} \right)^4 + \left(\pi \frac{\sigma_y \sigma_z}{R^2} \right)^3 \right]^{1/3}} . \qquad (11)$$

Each of these terms is consistent with fundamental physical relations that have been developed and verified over the past two decades. For example, note that in the limit of $x \rightarrow 0$ for zero plume buoyancy ($F_{**} = 0$), the solution reduces to $CuR^2/Q = 3$, which is the well-known relation used in the ASHRAE (1993), Schulman and Scire (1993), and Wilson (1995) model for passive plumes well-mixed across the recirculation cavity just downwind of the building. Also, in the limit of very large x, the solution reduces to $Cu/Q = (\pi\sigma_y\sigma_z)^{-1}$, which is the well-known Gaussian plume model (where the receptor is on the plume centerline and the release is at ground-level). The σ_y and σ_z formulas are based on Briggs' equations as presented in Hanna et al. (1982).

Since the second term in the brackets describes the growth of the recirculation cavity, we assume that its growth should be capped at a distance of $50H_B$, which corresponds to the distance at which Hosker (1984) states that the effects of the cavity are dissipated. Similarly, because the third term describes the growth of the plume due to its buoyancy, its value is capped at a distance of $49F_o^{5/8}$, the distance to final plume rise as recommended by the EPA (1995) in the ISC3 User's Guide, where F_o has units m^4/s^3 and distance has units m. Briggs (1984) suggests some alternate formulas for calculating the distance to final plume rise, but these newer theoretical formulas have not yet been adopted in EPA regulatory models such as ISC3. Furthermore, some slight discrepancies may occur because these plume rise formulas are most valid for point sources, while the GDP sources may be better represented by line or area sources. The effects of these simplifications could be investigated in future sensitivity studies.

It is noted that the $\exp(-6F_{**}^{0.4})$ term in Eq. (11) can be thought of as a "buoyant lift-off" term, which describes the decrease in ground-level concentration, C_c, due to buoyant stretching or lifting of the plume. The initial buoyancy flux, F_o, is assumed to be conserved in the theoretical analyses. In the case of the GDP process buildings, the buoyancy flux used to define F_{**} should be f_cF_o because only part of the plume is assumed to be trapped in the cavity. The four terms in the brackets account for dilution across the area of the building face (at $x = 0$), further dilution as the cavity expands somewhat with downwind distance, additional dilution due to the growth of the buoyant plume, and passive dilution, respectively. Hall and Waters' (1986) observations suggest little change in the ground-level concentrations at downwind distances, x/H_b, of 1.2, 12, and 40, whether the plume is released from the upwind face, the downwind face, or the roof of the building.

As stated in Sect. 2, there is always positive buoyancy being emitted from the vents at the GDPs. Even in the absence of accidental UF_6 plumes, these vent plumes will be entrained into the recirculation cavity and will diffuse according to Eq. (11). When we consider only the UF_6 emissions and associated buoyancy flux from a few of these vents in Eq. (11), the lift-off effect [the $\exp(-6F_{**}^{0.4})$ term] will be conservative because in reality, the F_0 term should include the buoyancy from all vents. Consequently, the concentration predictions with Eq. (11) are also conservative.

Note that Eq. (11) uses Wilson's (1995) suggestion that the scaling area in the recirculation cavity is given by $R^2 = H_B^{4/3}W_B^{2/3}$, rather than H_BW_B, where W_B is set equal to $8H_B$ if $W_B > 8H_B$. R is the representative scaling length for the building. For the GDP process buildings, where $W_B = 10H_B$, R is about $2H_B$. For the GDP transfer buildings, where $W_B \approx 2H_B$, R is about $1.3H_B$. This change results in conservative predictions of concentration for buildings with large aspect ratios because it is implied that the plume does not mix uniformly across the full width of the wake.

Equation (11) has the desired traits of agreeing with Wilson's (1995) formula for a well-mixed recirculation cavity at the downwind edge of a building, with Briggs' (1995) formula for buoyant plumes in the near and far cavity regions, and with the standard Gaussian passive gas plume formula at large distances. It is noted that, for strongly buoyant plumes, when F_{**} is the largest and lift-off is important, the plume rise will be relatively large, and the plume will be more likely to rise above the recirculation wake. Consequently, the fraction f_c of plume material trapped in the recirculation wake will be relatively small, and hence, C_c will also be small.

In the revised HGSYSTEM/UF_6 code, the prediction of C_c by Eq. (10) [the Wilson (1995) model for vent plumes trapped in wakes] is compared with the prediction of C_c by Eq. (11) without the lift-off term, $\exp(-6F_{**}^{0.4})$. In order to be conservative, the maximum value of these two alternate predictions of C_c is chosen. Then the lift-off term, $\exp(-6F_{**}^{0.4})$, is applied to the chosen value of C_c. It should be recalled that Eqs. (10) and (11) apply only to the fraction, f_c, of the plume caught in the recirculation cavity of the building. Consequently, the total source emissions, Q, and the total buoyancy flux, F_o, are multiplied by f_c before being applied to these equations.

4.3.1 Evaluations of Eq. (11) with Observations and Sensitivity Studies

As stated above, Eq. (11) was derived so that it provides a conservative best-fit to the wind-tunnel observations reported by Hall and Water (1986) and Hall et al. (1995). The tendency towards conservatism is shown in Fig. 4.1, on which the model predictions and the Hall and Waters (1986) observations are plotted in the form of non-dimensional concentrations, CuR^2/Q, as a function of non-dimensional buoyancy flux, $F_{**} = F_o/u^3W_B$. Observations were taken at three downwind distances (x = 60 m, 600 m, and 2 km, full-scale) and two surface roughnesses (z_0 = 0.2 m and 0.6 m, full-scale). It is seen that the model follows the general trend of the observed curves and is usually within about $\pm 20\%$ of the observations. The model is also nearly always conservative, except for slight (10 or 20%) underpredictions for three of the 24 points on the figure. Similar results can be seen for the Hall and Waters (1986) data for alternate building shapes (W_BH_B ranging from 1.0 to 3.0) and for wind angles off-perpendicular, and for the Hall et al. (1995) data for a variety of building shapes, wind angles, and numbers and locations for vents [these latter figures are not included here, but are available in the Briggs (1996) letter].

Several sensitivity studies were carried out in order to investigate the variations of the predictions of the model in Eq. (11) for a variety of input conditions (i.e., building shapes and stability classes). As an example of the results of one of these sensitivity studies, Fig. 4.2 shows the solution for two different choices of ambient stability class [neutral (D) versus stable (F)]. Stability class influences Eq. (11) only via the last terms, where the σ_y and σ_z formulas (from Hanna et al., 1982) are functions of stability class. The last term provides an asymptotic approach of the solution to the simple Gaussian plume model, and hence is most important at large downwind distances and small buoyancy fluxes. This expectation is borne out in Fig. 4.2, which shows very little effect of the stability class change at x = 60 m or 600 m, but a factor of two change at x = 2 km for small F_{**}.

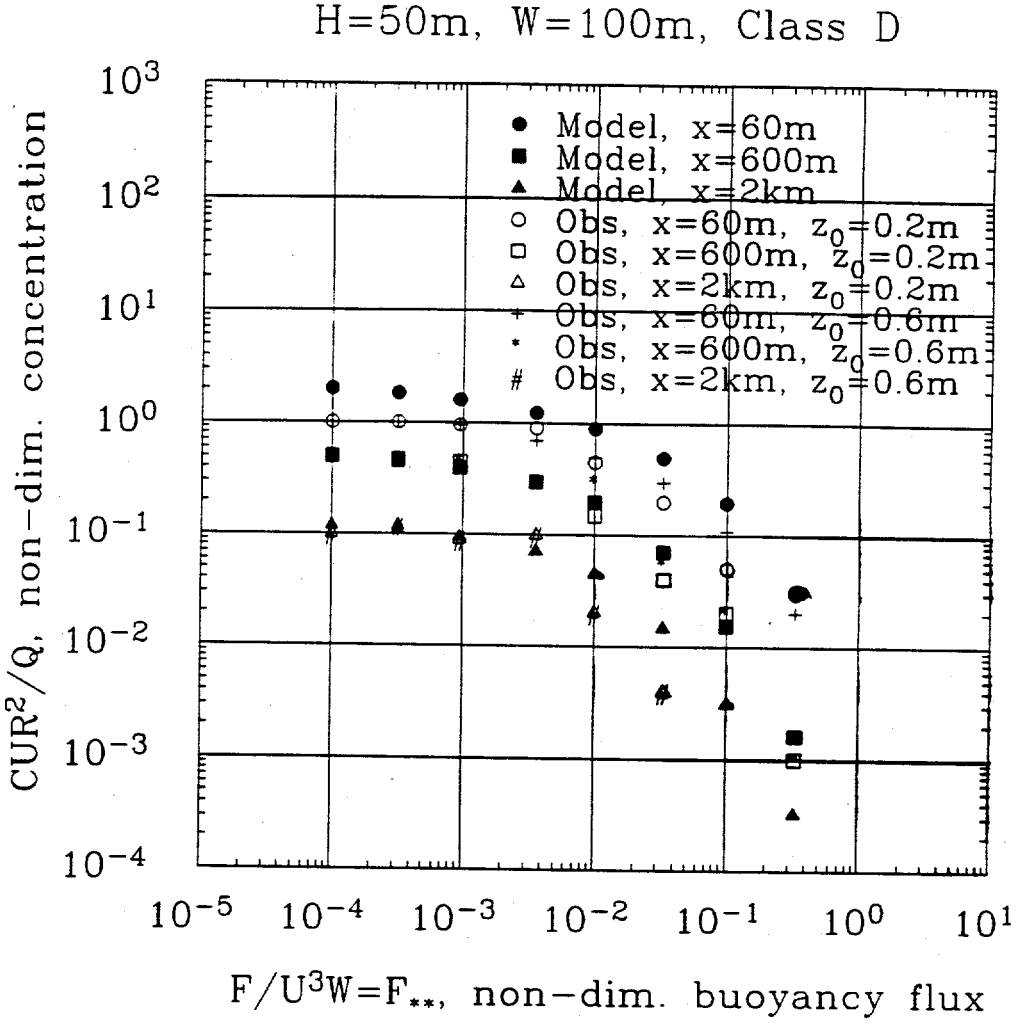

Fig. 4.1. Predictions of the model in Eq. (11), compared with observations in Hall and Waters' (1986) wind tunnel studies.

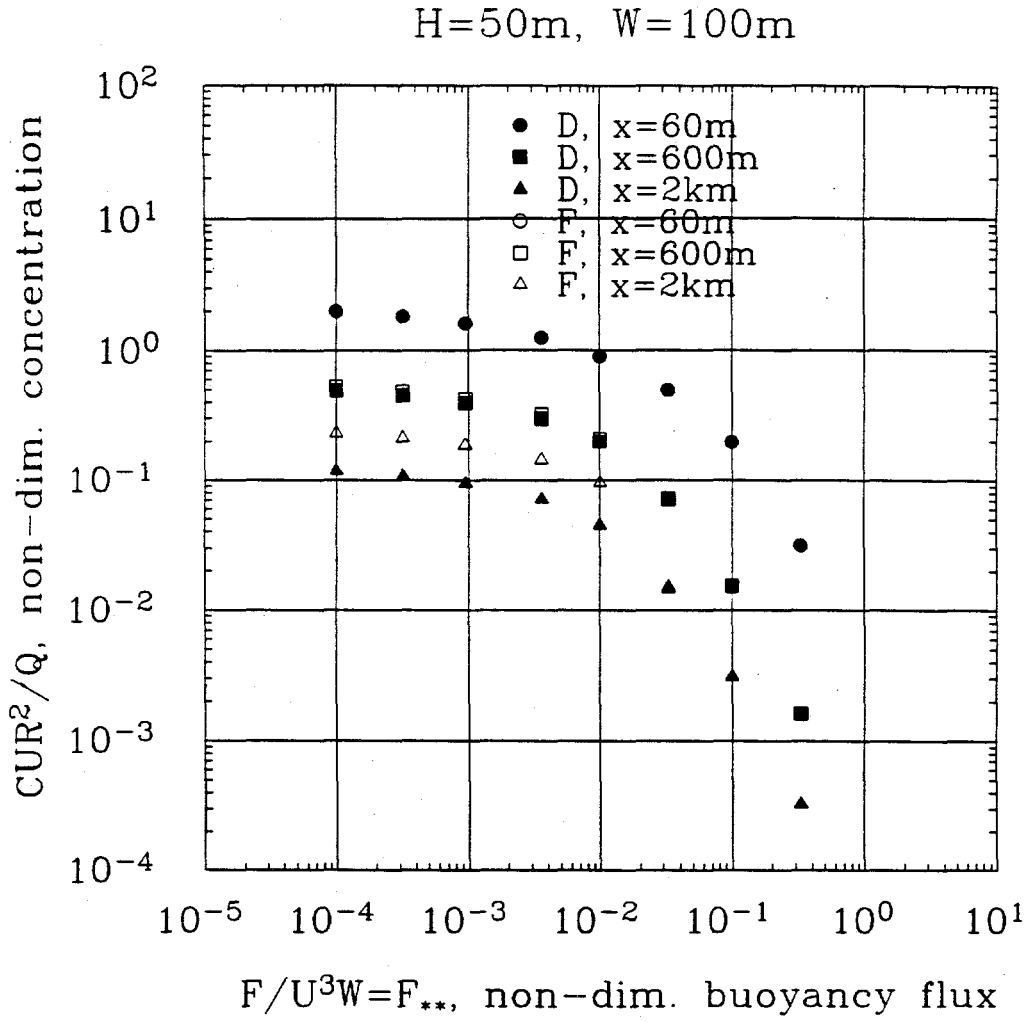

Fig. 4.2. Sensitivity study of the model in Eq. (11) for two different stability classes (D and F).

4.3.2 Comments on Conservatism

As stated previously, the use of the width, W_B, in the definition of F_{**} leads to conservative estimates of concentration for buildings that are short and wide, such as the GDPs. Another degree of conservatism is that the F_{**} term ignores the contribution of warm vent plumes that are entrained into the recirculation cavity but do not contain UF_6 products. Also, the method is conservative for the case of plumes that are released in the absence of buildings because the single term $\exp(-6F_{**}^{0.4})$ is applied to those plumes, without including the additional dilution effects of the F_{**} term in the denominator of Eq. (11).

4.4 Concentration Formulas for Part of a Plume above the Recirculation Cavity of a GDP Process Building

For the fraction, $1-f_c$, of the plume that remains ***above*** the recirculation cavity or wake, the EPA's (1995) ISC3 model is used to calculate the contribution to concentrations at ground-level. ISC3 is run with the building present. The source term for the part of the plume above the wake is $(1-f_c)\ Q$. The buoyancy flux is not reduced, however because the plume rise should not be changed from that used to calculate the plume centerline elevation, h_c, in Eq. (6). In addition, it should be noted that because the ISC3 code does not calculate concentrations at downwind distances within the wake (i.e., at $x < 3H_B$, which is the length of the cavity assumed by the ISC3 model), we modified the code so that the concentration predicted at the end of the wake is assumed to be valid at distances, x, less than $3H_B$. That is, the predicted ground-level concentration is constant for $x \le 3H_B$.

4.5 Method of Combining Contributions from Parts of a Plume in and above the Recirculation Cavity for a GDP Process Building

The contributions from the two components of the plume (caught in the recirculation cavity, as described in Sect. 4.3, and above the cavity, as described in Sect. 4.4) are summed for any downwind distance:

$$C_{total} = C_c \text{ (caught in cavity)} + C \text{ (above cavity)}. \qquad (12)$$

Our sensitivity tests show that Eq. (12) is usually conservative (i.e., gives the maximum concentration) when compared with the predictions of the ISC3 model as applied in standard EPA regulatory mode, where the building recirculation cavity effects are automatically accounted for by empirical approximations. It should be noted that our model defaults to the standard EPA regulatory model, ISC3, for buoyant plume scenarios in which only a small fraction of the plume is caught in the building recirculation cavity.

The releases at GDPs would likely occur simultaneously from several roof vents and motor exhaust ducts. Multiple sources are easily handled in ISC3 and also in the code described in Sects. 4.3 and 4.4. The ISC3 model allows arbitrary lateral distribution for sources and receptors.

However, because the predictions of models for concentrations in the recirculation cavity are independent of the lateral position of the vent or duct, an implicit assumption is made that *all* sources and receptors are lined up along the wind direction when Eqs. (10) and (11) are used.

Note that the equations in this section assume that the plumes from GDP process buildings are steady-state over time periods of about 10 min or more. If the plume emission rate and buoyancy flux vary slowly over a time period of about 1 hour, these equations can be applied piecewise to time segments (e.g., 10 min) over which the inputs can be assumed to be constant (i.e., varying by $\pm$ 20% or less). If the release has a constant emission rate but lasts only a short duration (e.g., a few minutes), then the procedures described in Sect. 5.4 can be used to account for the effects of finite release duration. The procedures are implemented in the POSTWAKE postprocessor for the GDP process building scenarios (see Appendix A).

5. DISPERSION AND LIFT-OFF IN AND DOWNWIND OF THE RECIRCULATION CAVITY OF GDP TRANSFER BUILDINGS

The source scenarios for accidental releases of UF_6 from the GDP process buildings and transfer buildings are described in Sect. 2, and the modeling approach for the process buildings is described in Sect. 4. The modeling approach for the GDP transfer buildings is similar but reflects the following differences in the scenarios:

Characteristic	Process Building	Transfer Building
Building width to height ratio?	W_B/H_B = 10 to 20	W_B/H_B = 2 to 4
Chemical reactions completed in building?	Probably yes	Probably no
Mode of release from building?	Fan-driven vertical plumes from roof vents and motor exhaust ducts	Horizontal plumes drifting out open bay doors on building side
Duration of release?	about 1 hour or more	A few minutes
Initial height of release?	Building rooftop H_B for most scenarios except at $H_B/2$ for earthquake scenario	Ground-level

Because of these differences, it is necessary to modify the model discussed in Sect. 4 to account for (1) chemical reactions and thermodynamics effects in the plume after it leaves the transfer building and (2) the time variation of the release. Since chemical reactions may still be occurring in the plume after it leaves the building and enters the recirculation cavity, the HEGADAS model is run using a *local* value of plume buoyancy flux, F_0, which may vary with downwind distance.

5.1 Initial Mixing in the GDP Transfer Building

As discussed in Sect. 2, this accidental release scenario involves a pressurized liquid UF_6 release from a valve or pipe rupture during a transfer operation within the GDP transfer building. The jet of UF_6 entrains ambient air in the building, flows around various obstacles (e.g., tanks and pipes), and finally exits the building through the open bay doors, whose area can be as large as the area of the downwind face of the building. While the UF_6 plume is being mixed in the building, it reacts with the water vapor in the building. The water vapor is assumed to instantly react with the UF_6.

The in-building mixing is accounted for by assuming that the cross-sectional area of the plume when it exits the building is a fraction, f_A, of the area of the downwind face of the building, $W_B H_B$. This fraction, f_A, is to be specified by the user. As a maximum, f_A equals the ratio of the area of the open doors to the area of the downwind face of the building. It is further assumed that the speed, u_p, of the plume is a constant equal to the ambient velocity upwind of the building at an elevation of $H_B/2$. Therefore the volume flux, V_P, of the plume exiting the building is given by the expression

$$V_P = u_p f_A W_B H_B \quad . \tag{13}$$

This volume flux includes both original and secondary (reaction products) plume material and entrained air. When the plume volume flux, V_P, and the initial mass flux are known, the concentrations of UF_6, HF, $HF{\cdot}H_2O$, UO_2F_2, and H_2O in the plume, as well as plume temperature and density at the bay doors, are calculated by using the chemistry and thermodynamics routines in HEGADAS/UF_6 with an instantaneous reaction rate. Depending on the mass of UF_6 released, the conditions in the building, and the volume of the entrained air, the UF_6 may or may not be totally reacted by the time it leaves the building.

5.2 HEGADAS Applications in the GDP Transfer Building Recirculation Cavity For Plumes that are Dense as They Leave the Building

If not all of the UF_6 has reacted with water vapor, then the plume exiting the transfer building may be more dense than the ambient air. In this case, the plume size and other characteristics of the plume calculated from the initial mixing algorithm in Sect. 5.1 are used as inputs to the HEGADAS/UF_6 model, which is applied in the building recirculation cavity and beyond. If the plume concentration calculated by HEGADAS/UF_6 decreases to a value appropriate for a well-mixed cavity, a transition is made to the cavity model [Eq. (11)] described in Sect. 4.3. The length of the recirculation cavity, L_R, can be calculated from Eq. (5). We assume that this equation is valid even for buildings whose length is less than three times their height. The length, L_R, is found to equal about $2H_B$ for the GDP transfer buildings, where W_B/H_B is equal to 2 to 4. The effects of enhanced turbulence in the cavity are accounted for by assuming a B ambient stability class in HEGADAS because it has been found that Wilson's (1995) solution [i.e., the term $u_H x_s^2/16$ in Eq. (10)] is equivalent to a Gaussian solution as long as σ_y and σ_z are chosen for stability class B. If the HEGADAS solution is still being used at the end of the cavity (i.e., the HEGADAS concentrations are greater than those for a well-mixed recirculation cavity at $x = L_R$), HEGADAS continues to be used beyond the cavity but with the appropriate local ambient stability class (rather than stability class B, which is always assumed in HEGADAS for plumes within the cavity). As the plume density asymptotically approaches the ambient density, HEGADAS automatically transitions to a passive gas Gaussian plume model at large distances.

As the plume travels downwind, the predicted ground-based HEGADAS/UF_6 plume could become positively buoyant (i.e., the plume density could be less than the ambient air density) due to heat released by chemical reactions. Reductions in ground-level concentrations due to the resulting vertical stretching (lift-off) can be accounted for by multiplying by the exponential

buoyant lift-off term, $\exp(-6F_{**}^{0.4})$, in Eq. (11). Although the exponential expression was suggested by Briggs (1996) for use with buoyant plumes that conserve their buoyancy flux, F_o, we propose using it for plumes with time- or distance-varying buoyancy fluxes, as long as u_H is interpreted as the ***local*** plume advection speed and W_B is interpreted as the ***local*** plume width in the formula $F_{**} = F_o/u_H^3 W_B$. Note that we are making the assumption that the lift-off term, $\exp(-6F_{**}^{0.4})$, can be applied to a wide range of initially ground-based buoyant plumes to describe the reduction in ground-level concentrations due to local buoyant stretching in the vertical direction. Because of the absence of theoretical analyses or wind tunnel and field observations of the lift-off effect for plumes whose buoyancy flux is varying, we make no corrections for the effects of plume inertia (i.e., the history of the plume geometry and buoyancy flux). As new theories and data become available, these empirical formulas can be modified to reflect the observations.

Another modification was made to HEGADAS to better simulate entrainment of ambient air when the plume becomes buoyant. Because HEGADAS was primarily developed for heavy gases (as its name implies), it contained an overly-simplified entrainment formulation for buoyant plumes. This simplified formulation could cause excessive entrainment. To hold the entrainment rate within known ranges and be confident that it agrees with theories, the formulation was modified so that if the plume becomes buoyant, the entrainment rate is limited to that for neutrally-buoyant, passive plumes. This is a conservative correction.

For the transfer buildings, the concentration predicted by HEGADAS (modified by a lift-off term as described in the preceding paragraph) is compared with the concentration predicted by Eq. (11) (i.e., the Briggs lift-off model for plumes initially well-mixed in recirculation cavities), and the maximum of these two alternate predictions of concentrations should be selected. In the application of Eq. (11), a constant value of F_o is needed for use in the buoyant plume growth expression in the denominator. For this purpose, the buoyancy flux, F_o, is assumed to equal the buoyancy flux that would occur after all reactions are completed.

5.3 Applications of a Well-Mixed Cavity and Lift-Off Model for Plumes that are Buoyant as They Leave the GDP Transfer Building

If the plume exiting the transfer building is less dense than the ambient air (i.e., the plume is buoyant), which may occur if all of the UF_6 has reacted with water vapor, then the lift-off correction to Eqs. (10) and (11) in Sect. 4.3 (for the GDP process building) can be applied. The Wilson (1995) model [Eq. (10)] is used while the plume is relatively small compared with the wake dimensions, and a transition is made to the Briggs (1996) model [Eq. (11)] when the concentration predicted by Eq. (10) drops below that predicted by Eq. (11) [without including the $\exp(-6F_{**}^{0.4})$ term]. When the F_{**} is applied, the buoyancy flux, F_o, is assumed to equal the buoyancy flux that would occur after all reactions are completed.

Note that the Wilson (1995) and Briggs (1996) models for buoyant plumes are being applied in a consistent manner to both the process and transfer building scenarios. The procedures are generally valid for a wide variety of release scenarios from a wide variety of building geometries.

5.4 Methods of Accounting for Averaging Time and Finite Duration Releases

The concentrations predicted by the models described above are valid for steady-state plumes. The source conditions and ambient conditions are assumed to be reasonably constant (i.e., within a range of ± 20%) over a time period of 10 min or more. Also, the ambient conditions are assumed to be maintained over the time period required for the plume to travel from the source to the receptor position (for most applications, this travel time is several minutes).

The basic averaging time implicit in the predictions of the above models is 10 min. To convert the predicted concentrations from an averaging time of 10 min to another averaging time, T_a, the following power law is used:

$$C(T_a) = C(10 \text{ min}) \ (10 \text{ min}/T_a)^{0.2} \quad . \tag{14}$$

This formula was recommended for use as an option in the original HGSYSTEM/UF_6 code (Hanna et al., 1996). Note that T_a should not be allowed to drop below 18.75 s so that the predicted concentrations do not exceed those observed in field studies for averaging times approaching zero.

In any accidental release of UF_6, the time duration of the release, T_d, can be estimated by several methods, such as dividing the mass of UF_6 released by the average mass emission rate, or estimating the time required for mitigation methods to be applied. At a given receptor on the plume centerline at a given downwind distance, x, the total amount of time required for the plume to pass over the receptor may be longer than T_d due to the effects of along-wind dispersion (this total time can be assumed to equal $T_d + 2m\sigma_x/u_c$). The parameter σ_x is the along-wind dispersion, u_c is the advective speed of the ground-based cloud, and m is 1 or 2 (we use 2). The value of m determines the amount of the leading and trailing edges of the concentration vs time profile included. The amount included is 68% for $m = 1$ and 95% for $m = 2$. The correction for averaging time given in Eq. (14) should not be applied if T_a is much greater than $T_d + 2m\sigma_x/u_c$ because there would be no plume present over the receptor for at least some of the time period defined by T_a. Thus T_a in Eq. (14) should be constrained by the time, $T_d + 2m\sigma_x/u_c$.

The original HEGADAS code (Witlox et al., 1990) includes a postprocessor, POSTHS, that can correct the steady-state solution for the effects of the finite duration time of the release. POSTHS automatically calculates the along-wind dispersion coefficient, σ_x, which elongates the finite-duration cloud in the forward and backward directions. A new post-processor, POSTMIX, has been added to the code that estimates the actual exposure time or averaging time for a finite-duration cloud passing a certain receptor as the smaller of a specified time or $T_a = T_d + 2m\sigma_x/u_c$. The specified time may correspond to the maximum exposure time of the receptor as determined by the accident scenario. Note that σ_x increases with time, and u_c also increases with time as the depth of the cloud increases. POSTMIX contains a mathematical expression [Witlox et al., 1990, p. 8–63, Eq. (1)] for estimating the concentration at a receptor as a function of time, $C(x,t)$, which

can be used to calculate the peak averaged concentration over time T_a. POSTMIX also calculates an additional parameter, the toxic load:

$$\text{Toxic load } (x) = \int_{\left(\frac{x}{u_c}+\frac{T_d}{2}\right)-\frac{T_a}{2}}^{\left(\frac{x}{u_c}+\frac{T_d}{2}\right)+\frac{T_a}{2}} C^n(x,t)\,dt \quad , \tag{15}$$

where the power, n, has been determined by toxicologists. The value of n is found to be different for various chemicals [e.g., $n = 1$ for UF_6 and $n = 2$ for HF (McGuire, 1991)]. The toxic load is a parameter to compare equivalent health impacts for different averaging times. The time-averaged concentration is equivalent to $n = 1$. Instead of applying Eq. (19) directly, the toxic load is sometimes estimated as the product of the time-averaged concentration raised to the *nth* power times the exposure time. Note, that in Eq. (15), $x/u_c + T_d/2$ is the middle point of the spreading plume.

The above procedures are performed by POSTMIX, a postprocessor for the GDP transfer building scenario, and are also implemented in POSTWAKE, a postprocessor for the GDP process building scenario.

6. IMPROVEMENTS IN THE ROBUSTNESS OF NUMERICAL ALGORITHMS IN AEROPLUME/UF_6

6.1 Description of Problems with Existing Numerical Algorithms

As mentioned in Sect. 1, testing of the AEROPLUME/UF_6 model by the authors and by LMES engineers during the time period from January through August 1995 revealed that the program occasionally encountered numerical difficulties. These problems were sometimes found for cases when the plume was impacting the ground with a relatively steep angle (e.g., $>20°$ from the horizontal); while the plume was still relatively dense (e.g., the plume density was 30% higher than that of air); and while the atmosphere was very stable (e.g., stability class F with an ambient wind speed of 1 m/s). Other problems sometimes arose for broad, shallow, dense gas clouds at moderate distances (a few hundred meters) downwind during light-wind stable conditions. The original AEROPLUME model (Post, 1994b) also has these problems occasionally, even though it contains no special treatment for UF_6 thermodynamics and chemistry.

Two remedies were suggested by Post (1994b) to resolve the above numerical difficulties: (1) alter the input conditions to AEROPLUME slightly or (2) adjust the control parameters for the SPRINT numerical solver (Berzins and Furzeland, 1985) used by AEROPLUME to integrate a set of ordinary differential equations. The problem with the first approach is that it is difficult to find satisfactory physical explanations for why AEROPLUME would fail for one case but would run for another similar case. The problem with the second approach is that it is time-consuming to apply the trial-and-error procedure required to find an optimal set of control parameters for the SPRINT solver. It is found that the set of SPRINT control parameters that works for one troublesome case does not necessarily work for another case. Furthermore, even after a set of SPRINT control parameters has been chosen that enables AEROPLUME to run to completion, the SPRINT solver may still generate warning messages. These messages indicate that the solver is still having difficulties but that the problem has been handled internally by "restarts" in integration. It is important to note that each "restart" implies a slight increase in plume dilution. Thus, for a given scenario, the predicted concentrations may be slightly different (1 or 2% for about 100 restarts).

It is believed that the numerical difficulties in AEROPLUME/UF_6 (and in the original AEROPLUME) are caused by (1) the large number of equations (a total of 14, see Sect. 6.2) that must be simultaneously solved by the SPRINT solver, (2) the complex interface required to link the SPRINT solver to the AEROPLUME/UF_6 code, and (3) the discontinuities that exist in the system due to the way some physical phenomena are parameterized by AEROPLUME/UF_6 for different downwind regimes. As shown in Sect. 6.2, the number of governing equations can be reduced; the SPRINT solver, together with its complex interface to the AEROPLUME/UF_6 code, can be replaced by a more robust Runge-Kutta solver with a simpler interface; and some formulas for physical phenomena considered by AEROPLUME/UF_6 can be revised. These changes result in an updated AEROPLUME/UF_6 model, called AEROPLUME/RK, which is much more robust than the existing code and takes less computer time to run.

6.2 Method for Simplification of the Equation Set

The original AEROPLUME model is part of the HGSYSTEM modeling system developed by Shell Research (Post, 1994b). AEROPLUME is intended to be applied to aerosol jets. AEROPLUME uses the following 14 equations to describe plume dispersion. (The same equations are also used in AEROPLUME/UF_6.) Variables, such as the plume density and the plume temperature, in the equations below are updated at each time step by the thermodynamics module.

$$\dot{m} = A(D,z,\phi)\rho u \tag{16}$$

$$\dot{P}_x = \dot{m}\left[u\cos(\phi) - u_{atm}\right] \tag{17}$$

$$\dot{P}_z = \dot{m}\, u \sin(\phi) \tag{18}$$

$$\dot{E} = \dot{m}\left[H + \frac{u^2}{2} - H_{atm} - \frac{u_{atm}^2}{2}\right] \tag{19}$$

$$\frac{dP_{atm}}{ds} = -\rho_{atm}\, g \sin(\phi) \tag{20}$$

$$\frac{dT_{atm}}{ds} = \frac{dT_{atm}}{dz}\sin(\phi) \tag{21}$$

$$\frac{du_{atm}}{ds} = \frac{du_{atm}}{dz}\sin(\phi) \tag{22}$$

$$\frac{d\dot{m}}{ds} = \text{Entr} \tag{23}$$

$$\frac{d\dot{E}}{ds} = -\dot{m}\left[\frac{dH_{atm}}{dz} + u_{atm}\frac{du_{atm}}{dz} + g\right]\sin(\phi) \tag{24}$$

$$\frac{d\dot{P}_x}{ds} = -\mathit{Shear} - \mathit{Drag} - \mathit{Impact}\sin(\phi) \tag{25}$$

$$\frac{d\dot{P}_z}{ds} = -\mathit{Buoy} + \mathit{Foot} - \mathit{Impact}\cos(\phi) \tag{26}$$

$$\frac{dx}{ds} = \cos(\phi) \tag{27}$$

$$\frac{dz}{ds} = \sin(\phi) \tag{28}$$

$$\frac{dt}{ds} = \frac{1}{u} \tag{29}$$

where

s	=	displacement along the plume trajectory (m),
$\dot{m}$	=	total plume mass flux, including the entrained air (kg/s),
H	=	plume specific enthalpy (J/kg),
u	=	plume velocity along the plume trajectory (m/s),
D	=	effective plume diameter (m),
ϕ	=	plume inclination angle from the horizontal (radians),
u_{atm}	=	ambient wind speed (m/s),
P_{atm}	=	ambient pressure (Pa),
T_{atm}	=	ambient temperature (K),
$\dot{E}$	=	plume excess energy flux (J/s),
$\dot{P}_x$	=	horizontal plume excess momentum flux (kg m/s^2),
$\dot{P}_z$	=	vertical plume excess momentum flux (kg m/s^2),
x	=	plume downwind displacement (m),
z	=	plume centroid height (m),
t	=	plume travel time, (s),
A	=	plume cross-sectional area (m^2),
ρ	=	plume density (kg/m^3),
g	=	gravitational acceleration (m/s^2),
H_{atm}	=	specific enthalpy of the ambient air (J/kg),
ρ_{atm}	=	density of the ambient air (kg/m^3),
Entr	=	air entrainment rate per unit plume travel length (kg/s/m),
Shear	=	shear force per unit plume travel length (kg/s^2),
Drag	=	ground drag force per unit plume travel length (kg/s^2),
Impact	=	ground impact force per unit plume travel length (kg/s^2),
Buoy	=	buoyancy force per unit plume travel length (kg/s^2),
Foot	=	gravity slumping force per unit plume travel length (kg/s^2).

For more details the reader is referred to Sect. 5 of the Technical Reference Manual for HGSYSTEM (Post, 1994b). For example, Sects. 5.B.7 and 5.B.8 describe the parameterizations of the terms *Entr*, *Shear*, *Drag*, *Impact*, *Buoy* and *Foot*, appearing in Eqs. (23), (25), and (26). It is assumed that the plume velocity has no crosswind component. In the original AEROPLUME, Eqs. (16) through (29) (four algebraic and ten differential equations) are simultaneously solved by the SPRINT solver, where s is the independent variable and $\dot{m}$, H, u, D, ϕ, u_{atm}, P_{atm}, T_{atm}, $\dot{E}$, $\dot{P}_x$, $\dot{P}_z$, x, z, and t are the 14 dependent variables.

After reviewing the above equations in the original AEROPLUME model, we came to the conclusion that, since some of the 14 dependent variables are functions of others, it is possible to reduce the number of equations that must be solved. For example, because ambient variables such

as u_{atm}, P_{atm}, and T_{atm} are functions of the plume centroid height, z, there is no need to calculate these three ambient variables separately. As another example, once D, ϕ, and u are known, $\dot{m}$, $\dot{P}_x$, and $\dot{P}_z$ are also known, or vice versa. Finally, because the plume travel time, t, is not used within the program at all, there is no need to solve for it explicitly.

As a result, it is possible to simplify the original system of equations solved by AEROPLUME to a reduced set of six differential equations, consisting of Eqs. (23) through (28), with $\dot{m}$, $\dot{E}$, $\dot{P}_x$, $\dot{P}_z$, x, and z as the six primary dependent variables. As demonstrated below, the remaining eight dependent variables (H, u, D, ϕ, u_{atm}, P_{atm}, T_{atm}, and t) can be expressed as functions of the six primary dependent variables.

The vertical profiles of u_{atm}, P_{atm}, and T_{atm} are known functions of z. The plume inclination angle, ϕ, can be given by the expression below [from Eqs. (17) and (18)]:

$$\phi = \tan^{-1}\left(\frac{\dot{P}_z}{\dot{P}_x + \dot{m}\, u_{atm}}\right) \quad . \tag{30}$$

The plume velocity, u, is given by the formula [from Eqs. (17) and (18)]

$$u = \frac{\dot{P}_x + \dot{P}_z + \dot{m}\, u_{atm}}{\dot{m}\,(\cos(\phi) + \sin(\phi))} \quad . \tag{31}$$

Once u is known, the plume cross-sectional area, A, is given by Eq. (16), or

$$A = \frac{\dot{m}}{\rho\, u} \quad . \tag{32}$$

Since A is a function of ϕ, z, and D, it is therefore possible to calculate D given values of A, ϕ, and z, which are already known. Note that when the plume is in the "touchdown" stage, this step involves solving a nonlinear equation that accounts for the assumed complex plume geometry, that is, a circular segment [Post, 1994b, p. 5-38, Eq. (17)]. The plume enthalpy, H, can be calculated by the expression [from Eq. (19)]

$$H = \frac{\dot{E}}{\dot{m}} - \frac{u^2}{2} + H_{atm} + \frac{u_{atm}^2}{2} \quad . \tag{33}$$

The plume travel time, t, can be approximated by a simple finite-difference method given below [from Eq. (29)]:

$$t = \sum_i \frac{s_{i+1} - s_i}{0.5\,(u_{i+1} + u_i)} \quad , \tag{34}$$

where the subscript I is the index for the integration step.

The AEROPLUME model requires the derivative of the plume inclination angle, ϕ, which is used to determine whether there is overlap of successive plume cross-sections [Post, 1994b, Sect 5.B.10]. As will be explained in more detail in Sect. 6.4.2, the purpose of this constraint was to preserve the integrity of the plume geometric system, which assumes that the plume cross-sectional plane is perpendicular to the plume centerline trajectory. Overlap of successive plume cross-sections may occur when the curvature of the plume centerline trajectory is large or when the plume diameter is large.

The AEROPLUME model also requires the derivative of the effective plume diameter, D, *when the plume is in contact with the ground* to parameterize (1) the gravity-slumping component of the air entrainment rate [Post, 1994b, Sect. 5.B.8] and (2) the gravity slumping force in Eq. (26) [Post, 1994b, Sect. 5.B.7]. The derivatives $d\phi/ds$ and dD/ds in AEROPLUME are directly calculated by the SPRINT solver because both ϕ and D are primary dependent variables. However, additional steps (described below) are necessary in AEROPLUME/RK to calculate $d\phi/ds$ and dD/ds because both ϕ and D are not directly solved for by the RKSUITE software package.

The derivative $d\phi/ds$ can be calculated by differentiating Eq. (30), knowing the values of the derivatives of $\dot{m}$, $\dot{P}_x$, $\dot{P}_z$, and u_{atm}. That is,

$$\frac{d\phi}{ds} = \frac{(\dot{P}_x + \dot{m}\, u_{atm})\, \frac{d\dot{P}_z}{ds} + \dot{P}_z \left(\frac{d\dot{P}_x}{ds} + \frac{d\dot{m}}{ds}\, u_{atm} + \dot{m}\, \frac{du_{atm}}{dz} \sin(\phi) \right)}{(\dot{P}_x + \dot{m}\, u_{atm})^2 + (\dot{P}_z)^2} \quad . \tag{35}$$

Because the plume cross-sectional area A is directly related to the effective plume diameter D, it would be expected that the derivative dD/ds could be estimated by taking the derivative dA/ds in Eq. (32). However, due to the highly nonlinear relationship between D and A for a circular segment in the "touchdown" stage [Post, 1994b, P. 5-38, Eq. (17)], the derivative dD/ds cannot be calculated as a straightforward analytic formula. Instead, it is suggested that dD/ds be estimated by a finite-difference expression similar to Eq. (38):

$$\frac{dD}{ds} \approx \frac{D_{i+1} - D_i}{s_{i+1} - s_i} \quad . \tag{36}$$

This approximation will be valid as long as the integration step is kept small in AEROPLUME/RK.

With the above approach, the equation system becomes simpler because the number of equations is reduced from 14 (differential and algebraic) to six (all differential). The original relations (or constraints) among the variables are still maintained, as expressed in Eqs. (30) through (33).

6.3 Discussions of the Runge-Kutta Solver

The SPRINT numerical solver (Berzins and Furzeland, 1985) is used in the existing AEROPLUME and AEROPLUME/UF_6 codes, as described by Post (1994b) and Hanna et al. (1997), respectively. The SPRINT solver is a software package used for solving systems of stiff or nonstiff differential equations coupled with algebraic equations (stiffness in a set of differential equations occurs when the independent variable exhibits two or more very different characteristic scales over which the dependent variables are varying). The SPRINT solver is incorporated in the widely used Numerical Algorithms Group (NAG) Fortran library. The code is quite complicated and its interface to the host program is complex.

As mentioned in Sect. 6.2, the original 14 (10 differential and 4 algebraic) governing equations used by AEROPLUME and AEROPLUME/UF_6 to describe plume dispersion have been reduced to 6 differential equations. Many "canned" solvers exist that can be applied to these six equations. These canned solvers are usually simpler to use than the SPRINT solver and are thus more robust. The relatively fast processes associated with chemical reactions of UF_6 and water vapor are not included in this equation set and are treated in separate thermodynamics and chemistry modules, as described by Hanna et al. (1996, Sect. 5). Thus, it is unlikely that the set of six differential equations used to describe plume dispersion possesses different time scales that would characterize a stiff system; therefore, because the system of equations is not stiff, there is no need to use a highly specialized solver such as SPRINT.

A number of software packages (or solvers) that perform integration for a set of ordinary differential equations were reviewed as candidates to replace SPRINT. The RKSUITE software package (Release 1.0, November 1991), was developed by scientists at the NAG in the United Kingdom and at Southern Methodist University in the United States. It was chosen after consideration of factors such as whether the code was easy to use, had been thoroughly tested, was well documented, and was in the public domain and could be redistributed without any licensing restrictions.

As the name implies, the RKSUITE software package is a suite of codes based on Runge-Kutta methods. Runge-Kutta methods are known for their robustness and usually succeed. The solution techniques used in the DEGADIS (Spicer and Havens, 1989) and SLAB (Ermak, 1990) models are also based on Runge-Kutta methods. Numerical errors are controlled in RKSUITE by automatic, adaptive step size control. The code decides what the optimal value for an internal step should be depending on how rapidly the dependent variables are changing. RKSUITE can also handle stiff equation sets, although excessive computer time might be required. If the solver determines that the equation set appears to be stiff, a warning message is generated, and the integration continues. Consequently, for a scenario when the equation set is stiff, the user will first be warned about the problem, and the solver will then proceed to generate as accurate results as possible. RKSUITE can be easily implemented because it has a much simpler interface to the host program than the SPRINT interface. RKSUITE calculates the derivatives of the primary dependent variables through direct function evaluation, whereas SPRINT achieves the same goal through the residual minimization technique.

The RKSUITE software package is designed to supersede some widely used similar codes, written by the same authors, which are available in the Sandia, Los Alamos, Air Force Weapons

Laboratory Technical Exchange Committee (SLATEC) and NAG Fortran libraries. The software package is available at many anonymous file transfer protocol (ftp) sites on the Internet. RKSUITE was obtained from the site *netlib.att.com* (i.e., AT&T's Bell Laboratories in New Jersey) under the directory */netlib/ode/rksuite*. The release notes (file *README*) and User's Guide (file *RKSUITE.DOC*) are also included in the AEROPLUME/UF_6 package. The new AEROPLUME/UF_6 code with the RKSUITE solver (replacing the SPRINT solver) is called AEROPLUME/RK.

6.4 Implementation of the Modified Equation Set and The Runge-Kutta Solver in AEROPLUME/RK

The implementation of the modified equation set and the Runge-Kutta solver RKSUITE in the new AEROPLUME/RK code must be modular so that the solution of the original AEROPLUME/UF_6 model can be duplicated and future upgrades to AEROPLUME/RK can be readily made. The parameterizations of physical phenomena in the new model must also be as consistent as possible with the original AEROPLUME and AEROPLUME/UF_6 models. These physical parameters include, for example, the air entrainment rate, the shear force, the ground drag force, the ground impact force, the buoyancy force, and the gravity slumping force [denoted as *Entr*, *Shear*, *Drag*, *Impact*, *Buoy*, and *Foot*, respectively, in Eqs. (23), (25), and (26)].

6.4.1 Review of the Original AEROPLUME

Before discussing the details of how the modified equation set and the RKSUITE solver have been implemented in the new AEROPLUME/RK model, it is useful to first review the solution procedure in the original AEROPLUME/UF_6 model. The original AEROPLUME/UF_6 model carries out the plume integration through a single call in its main program to the main driver routine PLMINT, which in turn performs the integration one step at a time along the plume trajectory by calling the SPRINT solver. PLMINT also calls the routine UF6 at the end of each integration step to perform the thermodynamics and chemistry calculations (Hanna et al., 1996, Sect. 5). Furthermore, a number of user-developed interface routines are also required so that SPRINT can be properly linked to AEROPLUME/UF_6. These routines perform the following tasks:

- Calculation of the residuals of Eqs. (16) through (29)
- Monitoring of the integration status of SPRINT
- Solving of the four algebraic Eqs. (16) through (29)
- Implementation of an artificial plume dilution and a restart in integration in case SPRINT encounters numerical difficulties
- Initial estimation of the derivatives of the 14 primary dependent variables

The driver routine PLMINT, together with all interface routines for the SPRINT solver, are collected in one Fortran file called PLUME.FOR. All generic library routines related to the SPRINT solver itself are collected in three Fortran files called SPRINT.FOR, SPGEAR.FOR, and SLINPK.FOR. The routines used to calculate values of the terms *Entr*, *Shear*, *Drag*, *Impact*, *Buoy*, and *Foot* in Eqs. (23), (25), and (26) are collected in one Fortran file called APMAIN.FOR.

6.4.2 Details of Implementation in AEROPLUME/RK

The details of implementation of the AEROPLUME/RK model are given below. The general approach will be discussed first. Descriptions of specific modifications will then be presented. The modifications include

- derivation of a more robust estimate of the rate of lateral plume spread,
- method of accounting for the constraint of no plume cross-section overlap,
- specification of optional control parameters for RKSUITE,
- generation of additional output, and
- correction for a coding error.

6.4.2.1 General approach

The original AEROPLUME/UF_6 model carries out the plume integration through a single call in its main program to the main driver routine PLMINT. The call to the routine PLMINT is disabled in the new AEROPLUME/RK code and is replaced by a call to the new driver routine called PLMINTRK. Like PLMINT, PLMINTRK (1) carries out the plume integration one step at a time by calling the RKSUITE solver and (2) calls the routine UF6 at the end of each integration step to perform the thermodynamics and chemistry calculations. If the call to PLMINTRK is disabled and the call to PLMINT is activated in AEROPLUME/RK, then the original SPRINT solver will be used to solve the original set of 14 governing equations, and AEROPLUME/RK will reproduce the results given by AEROPLUME/UF_6.

Most of the user-specified interface routines (see Sect. 6.4.1) in the original Fortran file PLUME.FOR could not be directly used and had to be redeveloped because the interface for the RKSUITE solver is different (and simpler) than the interface for the SPRINT solver. In fact, the RKSUITE solver requires only one interface routine for the evaluation of the right-hand sides of Eqs. (23) through (28). The main driver routine, PLMINTRK, the new interface routine, and other supporting routines (such as FDDDS and CKOVLP to be described later) were collected in a new Fortran file called PLMINTRK.FOR, which corresponds to PLUME.FOR in the original AEROPLUME/UF_6 code. All generic library routines related to the RKSUITE software package itself are collected in a Fortran file called RKSUITE.FOR, which corresponds to SPRINT.FOR, SPGEAR.FOR, and SLINPK.FOR in the original AEROPLUME/UF_6 code. (Note that RKSUITE.FOR was directly downloaded from the Internet, with minor changes to reflect the PC environment for which the AEROPLUME/RK code was developed.) The same routines that are in the original Fortran file APMAIN.FOR are still used in the new AEROPLUME/RK code for the terms *Entr*, *Shear*, *Drag*, *Impact*, *Buoy*, and *Foot* in Eqs. (23), (25), and (26). Some minor differences are described in the following subsection.

6.4.2.2 Derivation of a more robust estimate of the rate of lateral plume spread

The AEROPLUME model requires the derivative of the effective plume diameter, D, to parameterize (1) the gravity-slumping component of the air entrainment rate [Post, 1994b, Sect. 5.B.8] and (2) the gravity slumping force in Eq. (26) [Post, 1994b, Sect. 5.B.7]. In Sect. 6.2, it was first suggested that in AEROPLUME/RK the derivative dD/ds be approximated by the finite-difference method [Eq. (36)]. However, testing of the new AEROPLUME/RK code with a number

of cases that were known to cause numerical difficulties in the original AEROPLUME/UF_6 code showed that the problems with AEROPLUME/UF_6 (and the original AEROPLUME) were due in part to the fact that the distribution of the derivative *dD/ds* with distance, *s*, was not always smooth.

For example, there was usually a sudden increase in *dD/ds* when the plume first impacted the ground at a relatively steep angle (e.g., >20° from the horizontal) while the plume was still relatively dense (e.g., the plume density was 30% higher than that of air). This increase in *dD/ds* is physically realistic because the plume, while sinking toward the ground, would be suddenly under the influence of a rigid lower boundary. The gravity-slumping force, denoted by *Foot* in Eq. (26), is assumed to be proportional to the square of *dD/ds* [Post, 1994b, P.5-44, Eq. (32)]:

$$Foot = \left(\frac{3\pi^2}{32}\right)^3 \left(\frac{1}{k^2}\right) l\, \rho\, u^2 \left(\frac{1}{2}\frac{dD}{ds}\right)^2 , \qquad (37)$$

where l is the footprint width of the plume, ρ is the plume density, $k = 1.15$, and u is the plume velocity. If *dD/ds* were suddenly increased by a factor of 30 in 1 m of plume travel distance, which could happen when the plume first impacted the ground under the conditions just described, then the gravity-slumping force would be suddenly increased by the square of *dD/ds*, or by almost three orders of magnitude. The sharp increase in the gravity-slumping force expressed by Eq. (37) caused the less robust AEROPLUME/UF_6 code to fail. The more robust AEROPLUME/RK code is found to successfully handle this case. However, even though the predicted ground-level concentrations smoothly vary with downwind distance, the resulting variations with distance, *s*, of the predictions of the plume inclination angle and the plume centroid height may still not be smooth.

It is shown above that the rate of increase in plume diameter, *dD/ds*, may change rapidly when the plume first comes in contact with the ground. However, *dD/ds* may be further increased due to inconsistencies in the derivation of the gravity-slumping force [Eq. (37)] in the AEROPLUME model. According to Post (1994b, Sect. 5.B.7), the proposed formulation of the gravity-slumping force was originally based on the study by Raj and Morris (1987) for a slumped jet with a rectangular cross-section. The formulation was modified so that it was suitable for a plume with a semielliptic cross-section [leading to the factor $(3\pi^2/32)^3$ in Eq. (37)]. However, this modified formulation for the gravity-slumping force was then applied by AEROPLUME and AEROPLUME/UF_6 to cases when the plume had either a circular-segment or semielliptic cross-section.

A more robust estimate of the rate of lateral plume spread (i.e., the derivative *dD/ds*) is called for. Since the original formulation of the gravity-slumping force by Raj and Morris (1987) was for a ground-based rectangular jet, it is suggested that the formula for the rate of lateral plume spread should retain this geometrical relation. With a plume cross-sectional area, A, given by Eq. (32), an equivalent plume width, D', for a ground-based rectangular jet can be assumed:

$$D' = \frac{A}{2z} . \qquad (38)$$

Note that the plume height is twice the plume centroid height, z, for a ground-based rectangular jet. Differentiating Eq. (38) yields a revised estimate of the rate of lateral plume spread:

$$\frac{dD'}{ds} = \left(\frac{dA}{ds} - 2\, D' \sin\phi \right) \frac{1}{2z} \quad . \tag{39}$$

The derivative dA/ds can be estimated by a finite-difference approximation as

$$\frac{dA}{ds} \approx \frac{A_{i+1} - A_i}{s_{i+1} - s_i} \quad . \tag{40}$$

The revised estimate of the rate of lateral plume spread given by Eq. (39) is used in AEROPLUME/RK to calculate the gravity-slumping force in Eq. (37) and the gravity-slumping component of the air entrainment rate. Since dD'/ds is based on a rectangular plume cross-section, the factor $(3\pi^2/32)^3$ in Eq. (37) is no longer needed. The routine FDDDS is used to calculate the derivative dD'/ds in the AEROPLUME/RK code.

To evaluate the proposed formula for the rate of lateral plume spread, a test case has been created in which it is assumed that the release is a pure gaseous UF_6 jet, which is emitted in the downwind direction at a rate of 65.32 kg/s. The UF_6 is assumed to be released from a rupture whose diameter and elevation are 0.61 m and 6.92 m, respectively. The ambient temperature is 4.44°C, the ambient wind speed measured at 10 m is 1 m/s, and the atmospheric stability is class F. This test case was modeled by (1) AEROPLUME/UF_6, (2) AEROPLUME/RK with the gravity slumping force estimated by dD/ds in Eq. (36), and (3) AEROPLUME/RK with the gravity slumping force estimated by dD'/ds in Eq. (39).

Figures 6.1, 6.2, and 6.3 show the rate of lateral plume spread, the uranium concentration (mg/m^3), and the plume inclination angle (deg), respectively, predicted by the three AEROPLUME model options. All three model options predicted that plume touchdown occurred at a downwind distance of about 20 m. The uranium concentration and the plume inclination angle predicted by the three model options were virtually identical at downwind distances less than 20 m, that is, when the plume was airborne. The slight differences in the calculated rate of lateral plume spread at downwind distances less than 20 m were not relevant because that information is not used by the models when the plume is airborne. Figure 6.1 shows that immediately after plume touchdown the value of dD/ds predicted by AEROPLUME/UF_6 suddenly increased from 0.2 to 7.5. This factor of 37.5 increase in dD/ds, and the subsequent even larger increase in the gravity slumping force, caused AEROPLUME/UF_6 to fail. The two versions of AEROPLUME/RK also predicted a similar sudden increase in the rate of lateral plume spread immediately after plume touchdown. However, the highest values of the rate of lateral plume spread (4.3 for dD/ds and 2.9 for dD'/ds) were slightly smaller than that given by AEROPLUME/UF_6. It should be mentioned that because this test case involves a very dense jet that strikes the ground at an angle, it is physically realistic for the jet diameter to rapidly increase when it hits the ground. Both versions of the more robust AEROPLUME/RK code were successful in carrying out calculations beyond the region where the plume made a transition from the airborne stage to the touchdown stage.

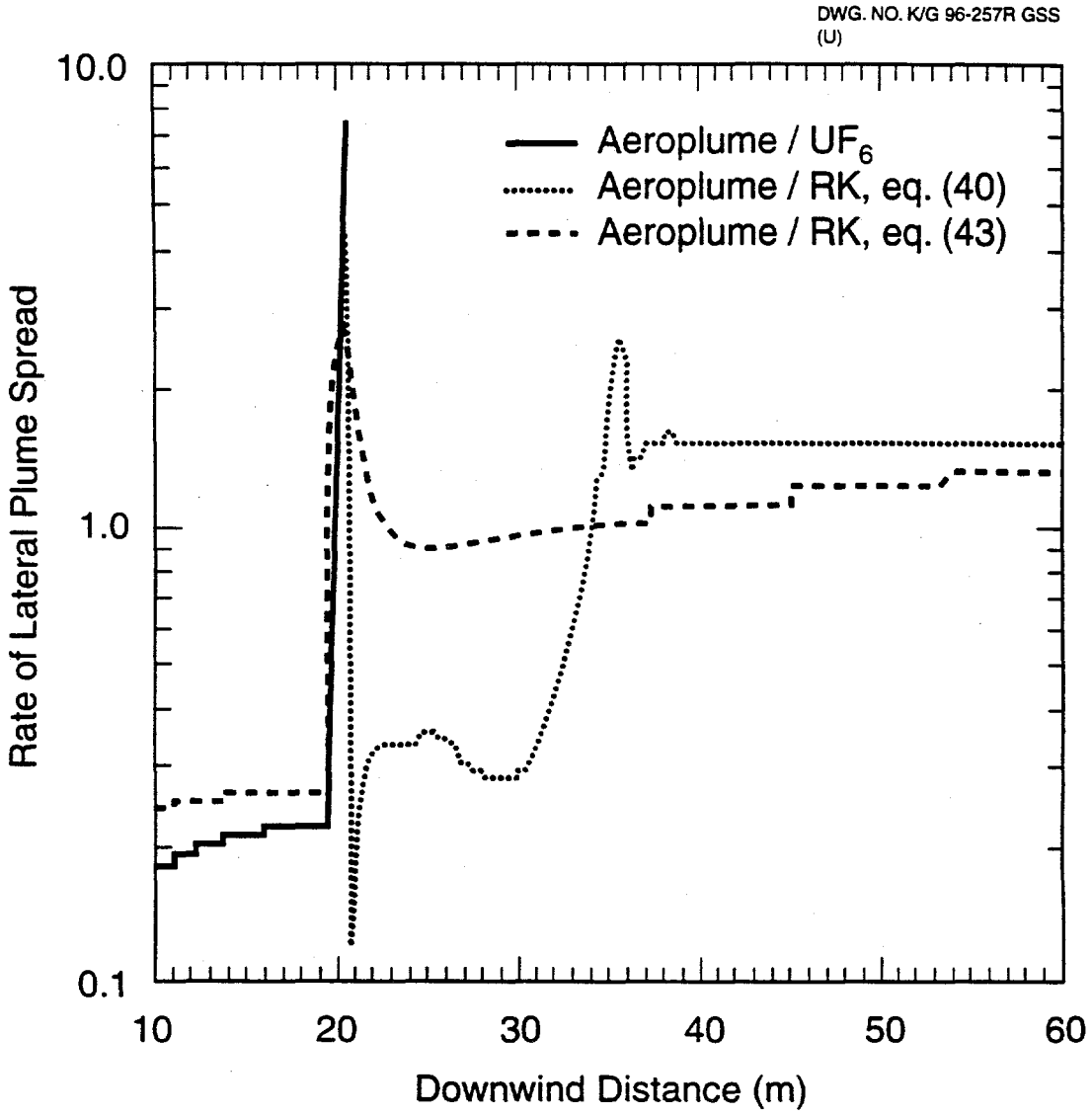

Fig. 6-1. Rate of lateral plume spread predicted by AEROPLUME/UF_6 (solid line), AEROPLUME/RK with *dD/ds* given by equation (36) (dotted line), and by AEROPLUME/RK with *dD'/ds* given by equation (39) (dashed). Plume touchdown occurs at a downwind distance of about 20 m. AEROPLUME/UF_6 encounters numerical difficulties at 20.3 m downwind.

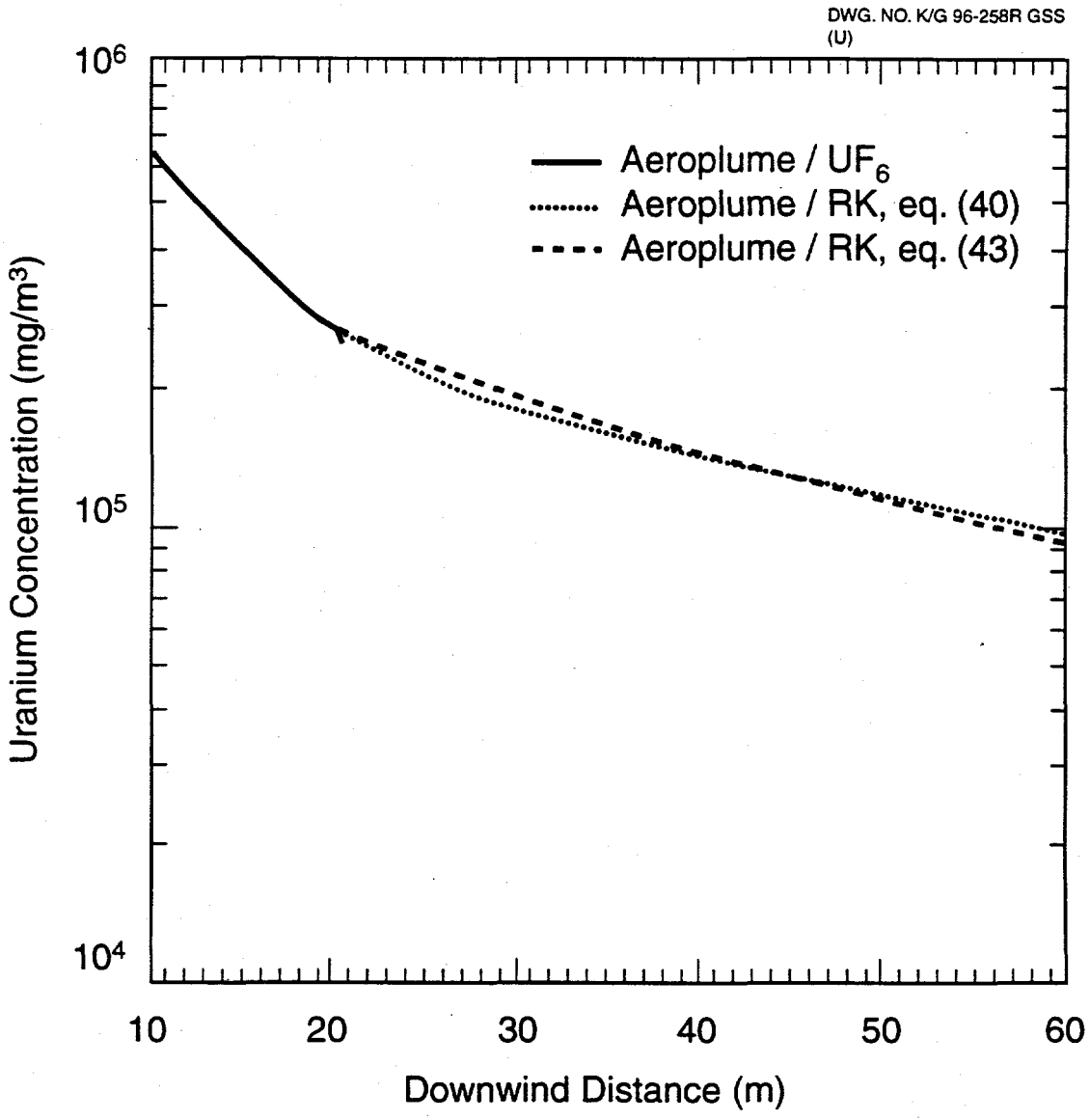

Fig. 6-2. Uranium concentration (mg/m^3) predicted by AEROPLUME/UF_6 (solid line), AEROPLUME/RK with *dD/ds* given by equation (36) (dotted line), and by AEROPLUME/RK with *dD'/ds* given by equation (39) (dashed line). Plume touchdown occurs at a downwind distance of about 20 m. AEROPLUME/UF_6 encounters numerical difficulties at 20.3 m downwind.

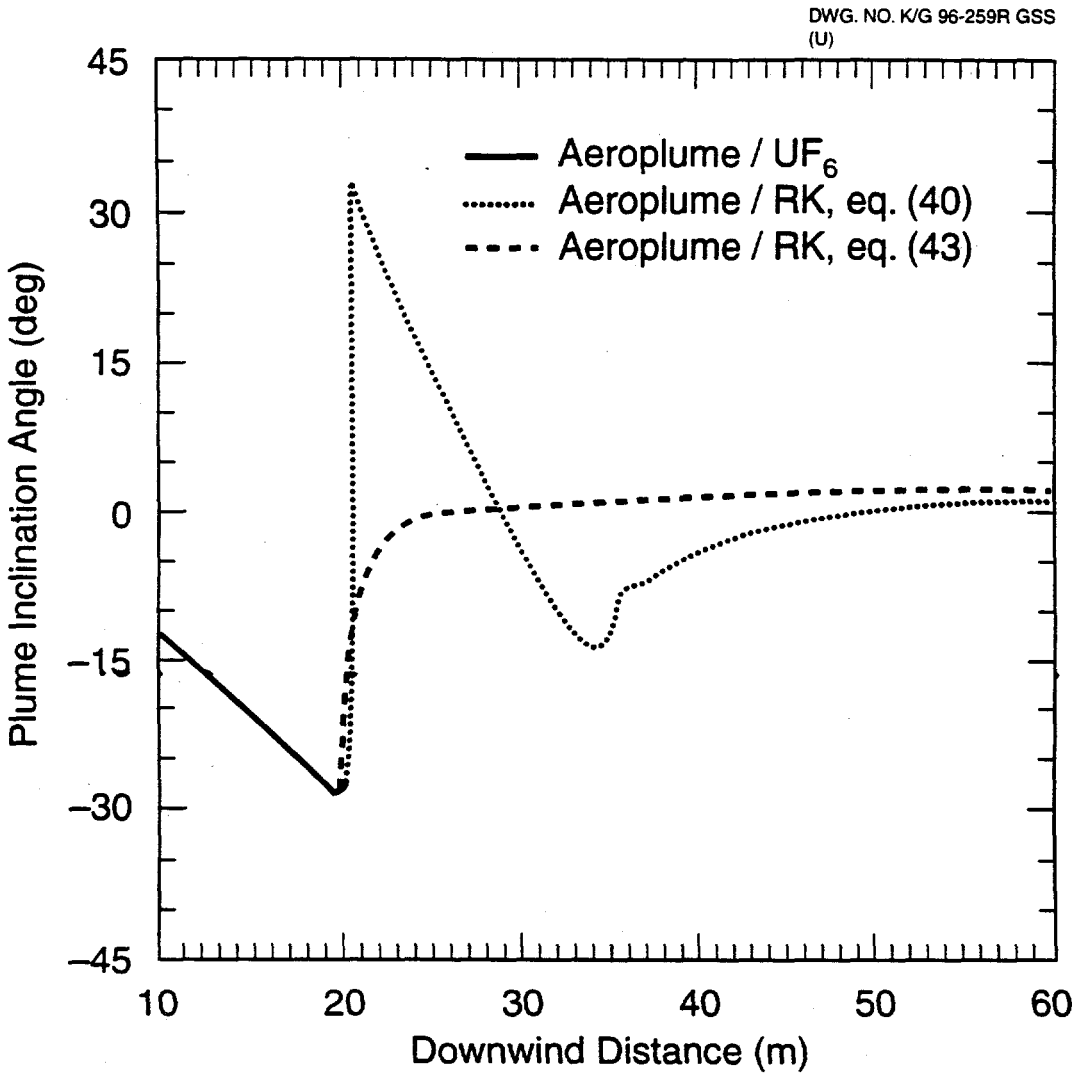

Fig. 6-3. Plume inclination angle (deg) predicted by AEROPLUME/UF_6 (solid line), AEROPLUME/RK with *dD/ds* given by equation (36) (dotted line), and by AEROPLUME/RK with *dD'/ds* given by equation (39) (dashed line). Plume touchdown occurs at a downwind distance of about 20 m. AEROPLUME/UF_6 encounters numerical difficulties at 20.3 m downwind.

It is seen from Fig. 6.1 that, while the rate of lateral plume spread given by *dD/ds* in Eq. (36) showed large variations at downwind distances between 20 and 36 m, the distribution of the rate of lateral plume spread given by *dD'/ds* in Eq. (39) was much smoother over the same region. The rates of lateral plume spread given by the two versions of AEROPLUME/RK gradually converged at large downwind distances. Despite the differences in the estimate of the rate of lateral plume spread, the two versions of AEROPLUME/RK yielded similar (within 5%) predicted uranium concentrations, as shown in Fig. 6.2. This is because the rate of lateral plume spread, and subsequently the gravity slumping force, mainly affected the plume trajectory but not the air entrainment rate. It can be seen from Fig. 6.3 that the plume trajectory predicted by AEROPLUME/RK was much smoother when *dD'/ds* was used.

6.4.2.3 Method of accounting for the constraint of no overlap of plume cross-sections

The original AEROPLUME and AEROPLUME/UF_6 models employed a constraint where the curvature of the plume trajectory was not allowed to exceed a limit determined by the condition that the successive plume cross-sections would "overlap." The purpose of this constraint was to preserve the integrity of the trajectory-following coordinate system for the plume. The conditions under which overlap of plume cross-sections would occur are shown below [taken directly from Sect. 5.B.10 of Post (1994b)].

For an airborne plume,

$$\frac{D}{2} \left| \frac{d\phi}{ds} \right| > 1 \quad ; \tag{41}$$

for a touchdown plume,

$$\frac{-z}{|\cos\phi|} \frac{d\phi}{ds} > 1, \qquad \text{for } \frac{d\phi}{ds} < 0 \quad , \tag{42}$$

$$\left[\frac{D}{2} - \frac{(z - z_c)}{|\cos\phi|} \right] \frac{d\phi}{ds} > 1, \qquad \text{for } \frac{d\phi}{ds} \geq 0 \quad ; \tag{43}$$

for a slumped plume,

$$\frac{-z}{|\cos\phi|} \frac{d\phi}{ds} > 1, \qquad \text{for } \frac{d\phi}{ds} < 0 \quad , \tag{44}$$

$$\left[\max(1, e) \frac{D}{2} - \frac{z}{|\cos\phi|} \right] \frac{d\phi}{ds} > 1, \qquad \text{for } \frac{d\phi}{ds} \geq 0 \quad , \tag{45}$$

where D is the effective plume diameter [not to be confused with D' in Eq. (38)], ϕ is the plume inclination angle, s is the displacement along the plume trajectory, z is the plume centroid height, z_c is the center height for a circular segment, and e is the plume eccentricity. Plume eccentricity is defined as

$$e = \frac{3\pi}{2} \frac{z}{D\,|\cos\phi|} \quad . \tag{46}$$

Figure 6.4 illustrates the condition under which plume cross-sections would overlap for an airborne plume. It is seen from Fig. 6.4 and Eqs. (41) through (45) that overlap of plume cross-sections can result from a steep curvature in the plume trajectory or from a large plume diameter.

To implement the constraint of no overlap of plume cross-sections, the AEROPLUME/RK code determines whether the above defined conditions of overlap of plume cross-sections are met at the end of each external integration step. If the plume cross-sections do happen to overlap, the value of ϕ is altered so that the value of the applicable expression equals 1.0 in Eqs. (41) through (45). Once ϕ is altered, some plume variables are also altered *in sequence* to ensure geometrical consistency. These include D, the effective plume diameter; P_x, the horizontal plume momentum flux; P_z, the vertical plume momentum flux; x, the plume downwind displacement; dD/ds; and $d\phi/ds$. Other plume variables such as the plume mass flux, the plume cross-sectional area, the plume centroid height, the plume velocity, the plume enthalpy, and the plume energy flux are assumed not to be affected by the constraint of no overlap of plume cross-sections. Since the variables ϕ, D, P_x, P_z, x, dD/ds, and $d\phi/ds$ are not simultaneously updated, the new solution might not lead to the applicable expressions being exactly equal to 1.0 in Eqs. (41) through (45). Consequently, the above procedure is iterated until a convergent solution is obtained. The calculations of overlap of plume cross-sections are in the routine CKOVLP in the new AEROPLUME/RK code.

6.4.2.4 Specification of optional control parameters for RKSUITE

When AEROPLUME/UF_6 is run, the user can specify, via an *optional* STP file for the SPRINT solver, the following values:

- the maximum internal integration step size,
- the minimum internal integration step size,
- the distribution of the external integration step sizes,
- the relative error tolerance for each of the 14 governing equations (i.e., 14 tolerance values are required), and
- the absolute error tolerance for each of the 14 governing equations (i.e., 14 tolerance values are required).

The control parameters specified in the STP file can be adjusted so that numerical difficulties encountered by AEROPLUME/UF_6 can be overcome (see Sect. 6.1).

The same optional STP file can be used to control how the RKSUITE solver performs integrations in the new AEROPLUME/RK code. However, only a few of the parameters specified in the STP file are actually used by AEROPLUME/RK because the RKSUITE solver has a simpler interface to the host program.

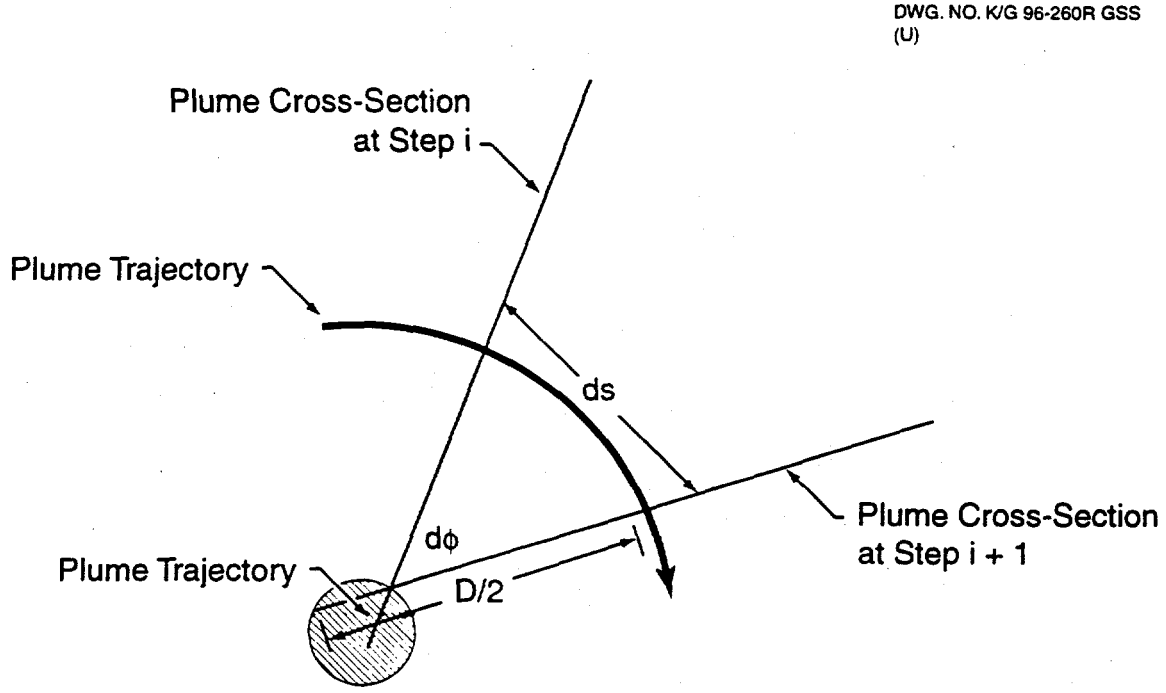

Fig. 6-4. Overlap of successive plume cross sections for airborne plume. D is the plume diameter, ϕ is the plume inclination angle, and s is the displacement along the plume trajectory. Overlap of successive plume cross sections can result from large curvature in plume trajectory or large plume diameter.

In particular, the following parameters are used:

- the minimum internal integration step size (treated by RKSUITE as the initial internal integration step size),
- the distribution of the external integration step sizes, and
- the first value of the relative error tolerances (applied by RKSUITE as the relative error tolerance for *all* six governing equations).

AEROPLUME/RK will use the default values specified in the code for the above control parameters if the STP file does not already exist. It is recommended that the option of specifying the control parameters for the RKSUITE solver via the STP file only be used by advanced users who are very familiar with the RKSUITE solver and the AEROPLUME/RK code. It is expected that the user will rarely have to adjust the control parameters for the RKSUITE solver in order to run AEROPLUME/RK because AEROPLUME/RK is more robust than AEROPLUME/UF_6.

6.4.2.5 Correction for two coding errors

In the original AEROPLUME model (Post, 1994b), there was a coding error in the calculation of the gravity-slumping force that accounts for the spreading of a plume after the collapse of gravity current. The error occurred in the statement

$$SLUMP = SLUMP*USTAR*DDDS*KAPPA*CFCPRW/RICF$$

in the routine SLUMP in the Fortran file APMAIN.FOR. The term *KAPPA* (= 0.41 in the code) in the above statement should be *CFVULD* (= 1.15 in the code). This coding error was corrected in AEROPLUME/RK.

An inconsistency between the Technical Reference Manual (Post, 1994b) and the original AEROPLUME code was found in the sign for the ground impact force in Eq. (26). The formulation in the Technical Reference Manual is believed to be correct because it leads to the ground always exerting an upward force to the plume regardless of the sign of the plume inclination angle, ϕ. The formulation in the original AEROPLUME code suggests that the ground will exert an upward force to the plume when the plume is descending ($\phi < 0$) and a downward force to the plume when the plume is ascending ($\phi > 0$). The AEROPLUME code was modified to make it consistent with the Technical Reference Manual.

6.4.2.6 Other changes related to making the code more robust

Three distinct plume stages, *airborne*, *touchdown*, and *slumped*, are simulated by the AEROPLUME model. The entrainment assumptions and the forces included in the plume momentum Eqs. (25) and (26) are different (or discontinuous) for three different stages. The discontinuities are most pronounced between the *airborne* and *touchdown* stages. The original AEROPLUME model allowed the plume stage to change only in one sequence: from *airborne* to *touchdown* to *slumped*. Once the plume was in the *slumped* stage, it could not switch back to other stages. This limitation was removed in the UF_6 version of AEROPLUME because the heat generated by the chemical reactions of UF_6 with water vapor could sometimes cause the plume to

become lighter than air and possibly lift off the ground (see Sect. 4.3). Sensitivity tests with AEROPLUME/UF_6 show that, after the initial occurrence of plume lift-off, the plume could sometimes oscillate between the *airborne* and *touchdown* stages. The mathematical rationale for this phenomena are described in the following paragraph.

In the original AEROPLUME code, the transition from *airborne* to *touchdown* stages occurs when

$$\frac{0.5\ D\ \cos(\phi)}{z} > 1.0 \quad , \tag{47}$$

where D is the effective plume diameter, ϕ is the plume inclination angle, and z is the plume centroid height. When AEROPLUME/UF_6 was first developed, the plume was allowed to switch from *touchdown* back to *airborne* if the transition criterion in Eq. (47) was not met. However, if the value of this expression happens to hover around 1.0, then the AEROPLUME/UF_6 code will predict that the plume will oscillate between the two stages, and the system will be subject to undesirable repeated occurrences of discontinuities. To prevent this, in the new AEROPLUME/RK code, the transition criteria between the two stages were modified. A transition from *airborne* to *touchdown* is assumed to occur when

$$\frac{0.5\ D\ \cos(\phi)}{z} > 1.02 \quad , \tag{48}$$

and a transition from *touchdown* to *airborne* is assumed to occur when

$$\frac{0.5\ D\ \cos(\phi)}{z} < 0.98 \quad . \tag{49}$$

An additional problem was found in the criteria used by the original AEROPLUME code to determine whether the model should make transition to one of the far-field models (HEGADAS or PGPLUME). The criteria were based on the velocity excess of the plume, the ratio of various components of air entrainment rates, and the relation between plume buoyancy and plume advection. For typical scenarios to be considered in the SAR, it is found that the AEROPLUME/RK code sometimes does not make the transition to a far-field model, even when all indications would suggest that the momentum effects of the jet have been dissipated. As explained below, this delay of the transition to the far-field model is primarily caused by the fact that the SAR cases are typically characterized by stable, light wind conditions. The transition criterion based on plume velocity excess can be expressed as

$$\left| 1 - \frac{u}{u_a} \cos(\phi) \right| < \text{RULST} \quad , \tag{50}$$

where u is the plume velocity, u_a is the ambient wind speed, ϕ is the plume inclination angle, and RULST is the threshold criterion (default = 0.1). For stable, light wind conditions where u_a is

small, it is relatively difficult to satisfy the above criterion. A solution to this problem is to develop another criterion based on *absolute* plume velocity excess. The following criterion has been added to the new AEROPLUME/RK model.

$$| u \cos(\phi) - u_a | < 0.5 \text{ m/s} \quad . \tag{51}$$

Furthermore, the transition criterion based on the ratio of various components of air entrainment rates has been disabled in the new AEROPLUME/RK model because the partitioning of the air entrainment rates into various components is arbitrary. The transition criterion based on the relation between plume buoyancy and plume advection has also been disabled in the new AEROPLUME/RK model because the theoretical justification for that criterion is not provided in the Technical Reference Manual (Post, 1994b).

With the modifications described in the previous two paragraphs, the AEROPLUME/RK model will make an earlier transition to the far-field models. This is not inconsistent with other models, such as DEGADIS (Spicer and Havens, 1989) and SAPLUME (Kaiser, 1993), where the jet module makes a transition to the area-source module *immediately* after the plume touches the ground.

6.5 Comparisons of Predictions of AEROPLUME/UF_6 and AEROPLUME/RK

The previous section describes the implementation of the modified equation set and the RKSUITE solver in the new AEROPLUME/RK code. In this section, the predictions of the original AEROPLUME/UF_6 and the new AEROPLUME/RK models are compared for three scenarios:

- Scenario 1: A case when both AEROPLUME/UF_6 and AEROPLUME/RK ran successfully.
- Scenario 2: A case when AEROPLUME/UF_6 encountered numerical difficulties, but AEROPLUME/RK ran successfully.
- Scenario 3: Two similar cases when AEROPLUME/UF_6 ran for one case but failed for the other, and AEROPLUME/RK ran successfully for both cases.

Scenario 1:

The input conditions for Scenario 1 are summarized below:

Source information

Emission rate	10 kg/s
Release diameter	0.01 m
Release height	2 m
Release direction	downwind
Release temperature	60°C
Pollutant composition	100% liquid UF_6

Meteorological information

Wind speed measured at 10 m	6 m/s
Temperature	20°C
Relative humidity	80%
Stability class	D

Figures 6.5 (a) through (c) show the uranium concentration, the plume temperature, and the plume centroid height predicted by AEROPLUME/RK and AEROPLUME/UF_6. The figures show that the predictions were close (within 1%) for this test case, in which the plume underwent airborne, touchdown, and slumped stages.

Scenario 2:

The input conditions for Scenario 2 are listed below. Note that the test case considered here is the same as the one used in Sect. 6.4 to evaluate the performance of a more robust estimate of the rate of lateral plume spread.

Source information

Emission rate	65.32 kg/s
Release diameter	0.61 m
Release height	6.92 m
Release direction	downwind
Release temperature	143.3°C
Pollutant composition	100% gaseous UF_6

Meteorological information

Wind speed measured at 10 m	1 m/s
Temperature	4.44°C
Relative humidity	60%
Stability class	F

The uranium concentration, the plume temperature, and the plume centroid height predicted by AEROPLUME/RK and AEROPLUME/UF_6 are shown in Figs. 6.6 (a) through (c). Both model versions predicted that plume touchdown occurred at about 20 m downwind. AEROPLUME/UF_6 encountered numerical difficulties immediately after plume touchdown, but AEROPLUME/RK continued to run to completion. The figures show that at downwind distances less than 20 m, both models gave identical results, and that at downwind distances beyond 20 m, the distributions of the solutions obtained by AEROPLUME/RK appeared to be smooth and follow the trend that was physically intuitive. For example, Fig. 6.6 (a) shows that the predicted uranium concentration decreased by a factor of about three between 20 and 60 m downwind, which is similar to Fig. 6.5 (a). Figure 6.6 (b) shows that the plume temperature was approaching the ambient temperature. Figure 6.6 (c) shows the gradual rise in the plume centroid height after 20 m downwind due to the entrainment of ambient air.

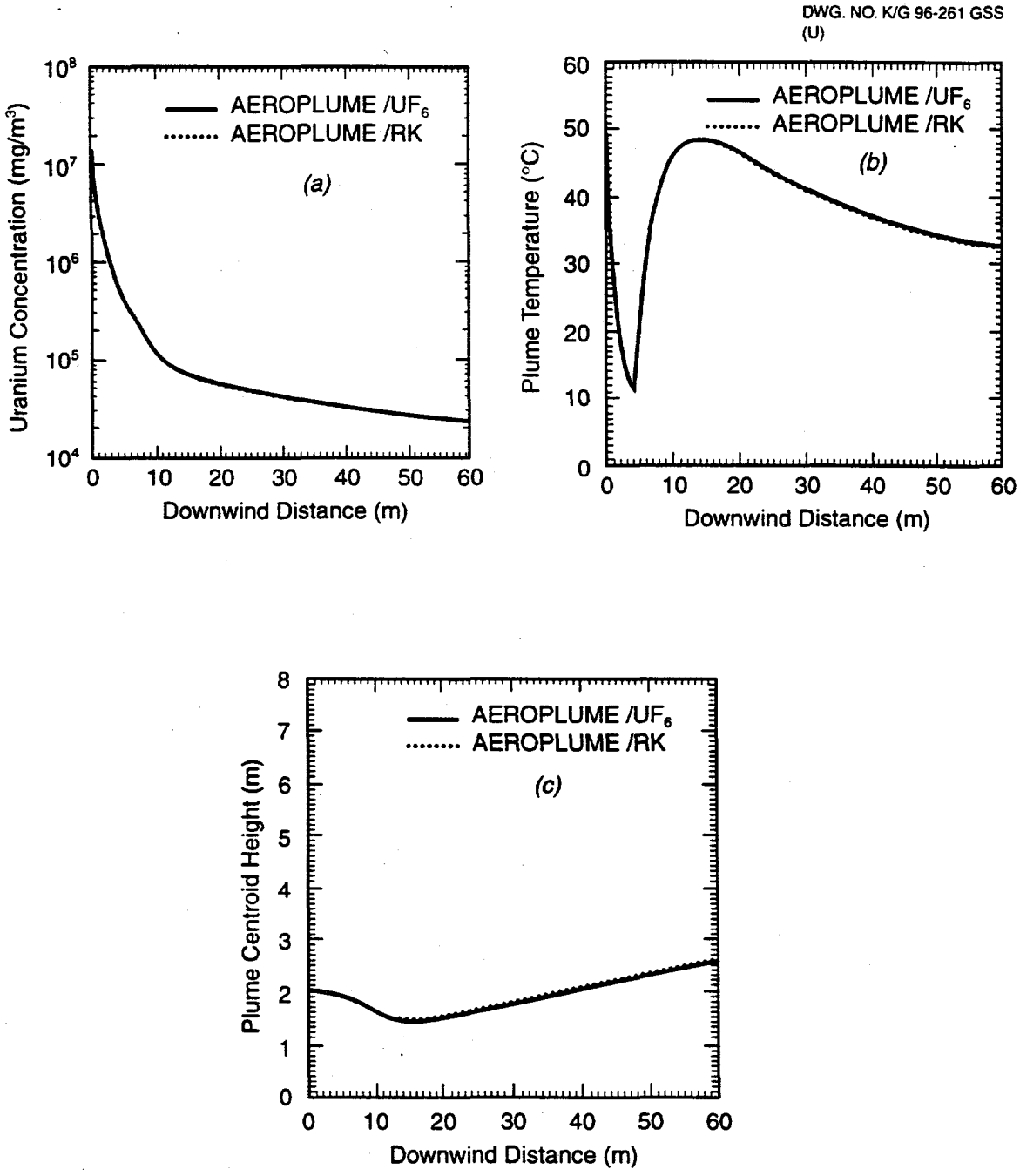

Fig. 6-5. Results predicted by AEROPLUME / UF_6 (solid lines) and AEROPLUME / RK (dotted lines) for Scenario 1. *(a)* Uranium concentration (mg/m^3). *(b)* Plume temperature (°C). *(c)* Plume centroid height (m).

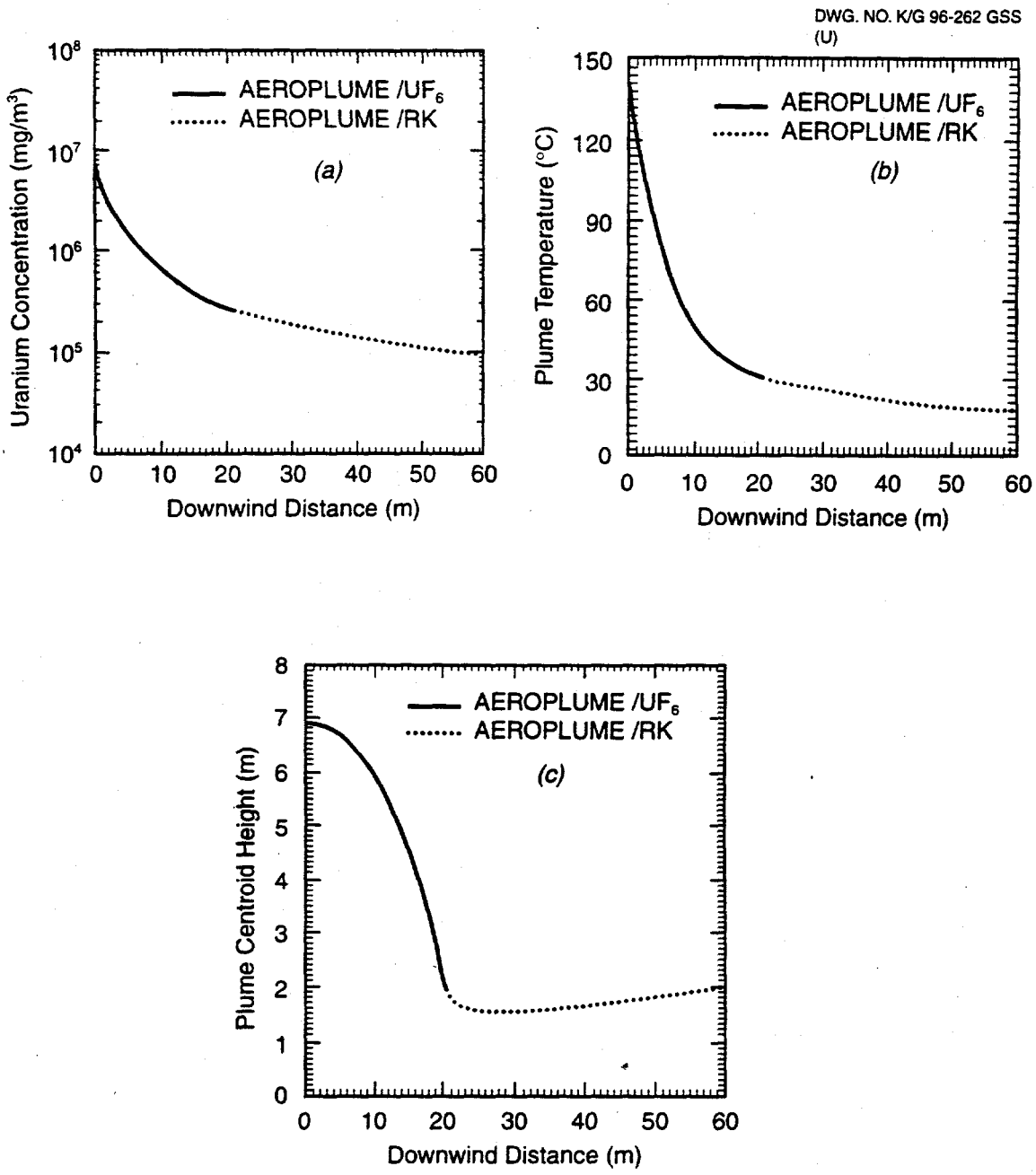

Fig. 6-6. Results predicted by AEROPLUME / UF_6 (solid lines) and AEROPLUME / RK (dotted lines) for Scenario 2. AEROPLUME/UF_6 encounters numerical difficulties at 20.3 m downwind. *(a)* Uranium concentration (mg/m^3). *(b)* Plume temperature (°C). *(c)* Plume centroid height (m).

Scenario 3:

Two similar test cases are considered for Scenario 3. The only differences between the two cases are the emission rate (6.66 kg/s vs 6.41 kg/s) and the release temperature (112.5°C vs 112.7°C). The input conditions for the two test cases are listed below.

Source information	**Case A**	**Case B**
Emission rate	6.66 kg/s	6.41 kg/s
Release diameter	0.0222 m	0.0222 m
Release height	6.71 m	6.71 m
Release direction	downwind	downwind
Release temperature	112.5°C	112.7°C
Pollutant composition	100% gaseous UF_6	
Meteorological information		
Wind speed measured at 10 m	1 m/s	1 m/s
Temperature	4.44°C	4.44°C
Relative humidity	60%	60%
Stability class	F	F

When AEROPLUME/UF_6 was applied to both cases, the model succeeded for case A but failed for case B. There is no good physical explanation for this failure because the model has difficulties with the case with the lower emission rate, which would be expected to exhibit less problems at the point where the dense plume reaches the ground. Figures 6.7(a) through (c) show the uranium concentration, the plume temperature, and the plume centroid height predicted by AEROPLUME/RK for cases A and B. As expected, AEROPLUME/RK yielded similar results for the two similar cases.

On the basis of the results presented above for Scenarios 1, 2, and 3, it can be concluded that AEROPLUME/RK produces results that are almost identical (i.e., differences generally less than 1%) to AEROPLUME/UF_6 for cases when AEROPLUME/UF_6 can run successfully. AEROPLUME/RK appears to be a robust model in cases where AEROPLUME/UF_6 encounters numerical problems. Furthermore, the run time for the new AEROPLUME/RK code is at least 50% less than that for the original AEROPLUME/UF_6 code.

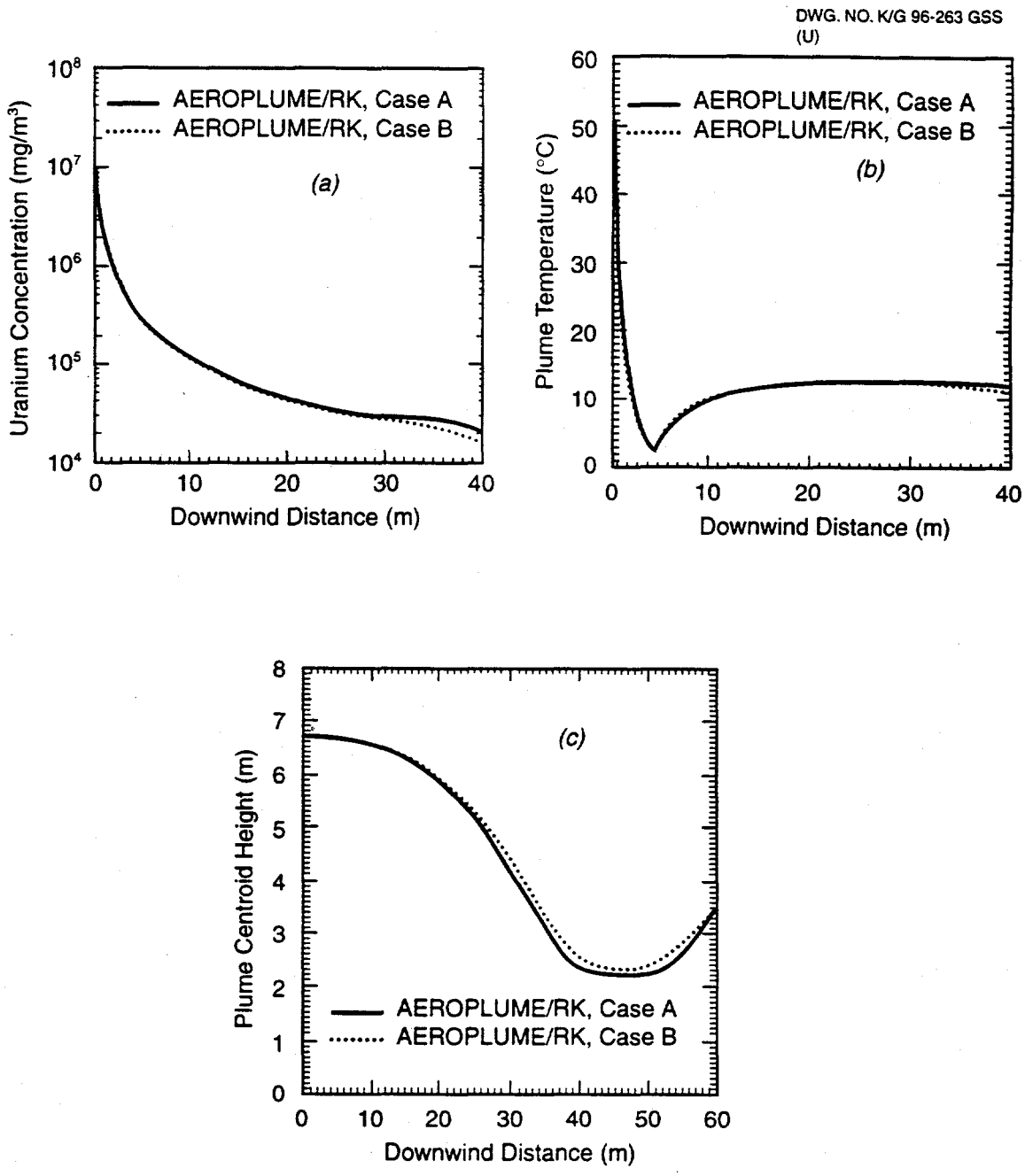

Fig. 6-7. Results predicted by AEROPLUME / RK for Case A (solid line) and Case B (dotted line) for Scenario 3. *(a)* Uranium concentration (mg/m^3). *(b)* Plume temperature (°C). *(c)* Plume centroid height (m).

7. SUMMARY OF MODIFICATIONS TO HGSYSTEM/UF_6 RECOMMENDED IN THIS REPORT

The HGSYSTEM/UF_6 model described by Hanna et al. (1996) has been modified to better account for dispersion and lift-off in and downwind of the cavity of GDP process and transfer buildings. The revised model is consistent with recent ASHRAE (1993) recommendations for the near-field dispersion of plumes from vents on buildings. After these small plumes dilute across the recirculation cavity behind the building, their further dilution and possible buoyant lift-off are treated using a new model proposed by Briggs (1996). This new model has been developed from fundamental physical principles and has been calibrated with wind tunnel observations by Hall and Waters (1986) and Hall et al. (1995). The two models described above have been shown to be conservative with respect to laboratory observations, and are designed to be conservative for building geometrics typical of GDPs (i.e., building widths are much greater than building heights).

The new modeling system also employs the EPA's ISC3 (1995) model for the portion of the plume that rises above the recirculation cavity. Thus, the system reduces to the standard regulatory model for situations with minimal influence of the building recirculation cavity.

In the case of plumes released through open side doors into the recirculation cavities of the transfer buildings at GDPs, it is necessary to specify the size of the plume as it leaves the building. If the plume size is small, some chemical reactions can take place after the plume enters the recirculation cavity. For contrast, for plumes released from vents on the process building of GDPs, it can be assumed that all reactions are completed. The revised model includes conservative assumptions wherever possible in these situations where input conditions are uncertain.

Another major modification involves the substitution of a more robust Runge-Kutta solver for the existing SPRINT solver in HGSYSTEM. This modification does not change the result, but merely assures that there will be a solution. Previously, users often had difficulties with the model "bombing," which led to extra trial-and-error efforts in an attempt to obtain a solution.

A final modification is the addition of formulas to account for the variations of concentrations with averaging time and to calculate the toxic load. These formulas are based on well-known relations in the literature.

REFERENCES

ASHRAE, 1993. "Air Flow Around Buildings." Chap. 14, *ASHRAE Handbook - 1993 Fundamentals*, American Society of Heating, Refrigerating, and Air-Conditioning Engineers, Inc., 1791 Tullie Circle, NE, Atlanta, GA 30329.

Berzins, M., and R.M. Furzeland, 1985. *A User's Manual for Sprint - A Versatile Software Package for Solving Systems of Algebraic, Ordinary, and Partial Differential Equations: Part 1 - Algebraic and Ordinary Differential Equations*, Report No. TNER.85.058, Shell Research Limited, Thornton Research Centre, U.K.

Briggs, G.A., 1973. *Lift-off of buoyant gas initially on the ground.* ATDL Cont. No. 87, RTDD/NOAA, Oak Ridge, TN 37831.

Briggs, G. A. 1975. "Plume Rise Predictions," Lectures on Air Pollution and Environmental Impact Analyses, D. A. Haugen (ed.), American Meteorological Society, Boston, Mass.

Briggs, G.A., 1984. "Plume Rise and Buoyancy Effects," *Atmosphere Science and Power Production*, DOE/TIC-27601, 327-366.

Briggs, G.A., 1995 (August 4). Letter to S.R. Hanna, EARTH TECH, Inc., Concord, MA 01742.

Briggs, G.A., 1996 (August 15). "Conservative re-fitting of lift-off equations." Letter to S. R. Hanna, EARTH TECH, INC., Concord, MA 01742.

Ermak, D.L., 1990. *User's Manual for SLAB: An Atmospheric Dispersion Model for Denser-than-Air Releases*.

EPA, 1995. *Users Guide for the Industrial Source Complex (ISC3) Dispersion Models, Vol. II—Description of Model Algorithms*, EPA-454/B-95-0036, U.S. Environmental Protection Agency, OAQPS, RTP, NC 27711.

Hall, D.J., C.F. Barrett and A.C. Simmonds, 1980. *Wind Tunnel Model Experiments on a Buoyant Emission from a Building*, Warren Spring Lab. Rep. No. LR 355 (AP), ISBN 0-85624-208-X, WSL, Gunnels Wood Rd, Stevenage, Hertfordshire, SG1 2BX, UK.

Goode, Jr., W. D., and R. W. Schmidt 1995. Lockheed Martin Energy Systems, Inc., Private communication to S. R. Hanna, EARTH TECH, Concord MA.

Hall, D.J. and R.A. Waters, 1986. *Further Experiments on a Buoyant Emission from a Building*, Warren Spring Lab. Rep. No. LR 567 (PA), ISBN 0-85624-425-2, WSL, Gunnels Wood Rd., Stevenage, Hertfordshire, SG1 2BX, UK.

Hall, D.J., V. Kukadia, S. Walker, and G. W. Marsland, 1995. "Plume Dispersion from Chemical Warehouse Fires." BRE Report CR 56/95, *Building Research Establishment*, Garston, Watford, WD275R, UK.

Hanna, S.R., G.A. Briggs and R.P. Hosker, Jr., 1982. *Handbook on Atmospheric Diffusion*, NTIS No. DE82002045 (DOE/TIC-11223), U.S. DOE TIC, Oak Ridge, TN 37831.

Hanna, S.R., J.C. Chang and J.X. Zhang, 1996. *Technical Documentation of HGSYSTEM/UF_6 Model*. DOE Report No. K/SUB/93-XJ947, available from OSTI, P.O. Box 62, Oak Ridge, TN 37831.

Hanna, S.R., J.C. Chang and J.X. Zhang, 1997. "Modeling Accidental Releases to the Atmosphere of a Dense Reactive Chemical (uranium hexafluoride)," *Atmos. Environ.* 31(6):901-908.

Hosker, R.P. Jr., 1984. "Flow and diffusion near obstacles." Chap. 7, *Atmos. Science and Power Prod.* NTIS No. DE84005177 (DOE/TIC-27601), (ed. by D. Randerson), Oak Ridge, TN 37831, 241-326.

Huber, A.H., 1989. "The Influence of Building Width and Orientation on Plume Dispersion in the Wake of a Building," *Atmos. Environ.*, **23**, 2109-2116.

Kaiser, G.D., 1993. *SAIC's Computer Programs for Modeling the Atmospheric Dispersion of Hazardous Vapors*; prepared for the U.S. Nuclear Regulatory Commission by Science Applications International Corp., 11251 Roger Bacon Drive, Reston, VA 22090

McGuire, S.A. 1991. *Chemical Toxicity of Uranium Hexaflouride Compared to Acute Effects of Radiation*, NUREG-1391, U. S. Nuclear Regulatory Commission, Washington, D.C.

Meroney, R.N., 1979. "Lift-off of Buoyant Gas Initially on the Ground," *J. Indust. Aerodyn.*, **5**, 1-11.

Post, L., 1994a. *An HGSYSTEM 3.0 User's Manual*, TNER.94.058, Shell Research Limited, Thornton Research Centre, P.O. Box 1, Chester, UK.

Post, L., 1994b. *An HGSYSTEM 3.0 Technical Reference Manual*, TNER.94.059, Shell Research Limited, Thornton Research Centre, P.O. Box 1, Chester, UK.

Raj, P.K., and J.A. Morris, 1987. *Source Characterization and Heavy Gas Dispersion Models for Reactive Chemicals*, AFGL-TR-88-0003(I), Technology & Management Systems Inc., Burlington, MA 01803-5128.

Schmidt, R. W., 1995 (Oct. 10 and Nov. 3). Lockheed Martin Energy Systems, Inc., memos to S. R. Hanna, EARTH TECH, Inc., Concord, MA 10742.

Schulman, L.L., S.R. Hanna and R.E. Britter, 1990. *Effects of Structures on Toxic Vapor Dispersion*. Report ESL-TR-90-99, HQ AFESC/RDVS, Tyndall Air Force Base, FL 32403.

Schulman, L.L. and J.S. Scire, 1993. "Building Downwash Screening Modeling for the Downwind Recirculation Cavity," *J. Air and Waste Manage Assoc.*, **43**, 1122-1127.

Slawson, P.R., G.J. Hitchman, and L.E. Hawbler, 1990. "The Characteristic Behavior of Finite Length Line Sources of Heat in a Crossflow," *J. Heat Transfer*, **112**, 349-355.

Spicer, T.O., and J.A. Havens, 1989. *DEGADIS Model - Version 2.1 User's Guide*, EPA/SW/DK-90/034a; prepared for EPA, Research Triangle Park, NC.

Wilson, D.J., 1979. "Flow Patterns Over Flat-Roofed Buildings and Applications to Exhaust Stack Design," *ASHRAE Transactions*, **85(2)**, 284-295.

Wilson, D.J. and R.E. Britter, 1982. "Estimates of Building Surface Concentrations from Nearby Point Sources," *Atmos. Environ.*, **16**, 2631-2646.

Wilson, D.J. and B.K. Lamb, 1994. "Dispersion of Exhaust Gases from Roof-Level Stacks and Vents on a Laboratory Building," *Atmos. Environ.*, **28**, 3099-3111.

Wilson, D.J., 1995. *Numerical Modeling of Dispersion from Short Stacks - Seminar 14: Accuracy and Realism of ASHRAE Handbook Estimates of Exhaust Gas Contamination of Nearby Air Intakes*. ASHRAE, 1791 Tullie Circle, NE, Atlanta, GA 30329.

Witlox, H.W.M., K. McFarlane, F.J. Rees, and J.S. Puttock, 1990. *Development and Validation of Atmospheric Dispersion Models for Ideal Gases and Hydrogen Fluoride, Part II - HGSYSTEM Program User's Manual*, TNER.90.016, Shell Research Limited, Thornton Research Centre, P.O. Box 1, Chester, UK.2

Appendix A

User's Guide for Revised HGSYSTEM/UF_6 Modules

A. User's Guide for Revised HGSYSTEM/UF_6 Modules

New HGSYSTEM/UF_6 modules (or models), including WAKE, POSTWAKE, UF_6MIXER, and POSTMIX, were developed in order to account for the effects of building wakes on plume rise and dispersion, and the effects of plume lift-off. The WAKE and POSTWAKE models, together with the ISCST3 model, are used to simulate releases from roof vents and stacks on the GDP process building, where releases are assumed to be buoyant but passive (inert). The UF_6MIXER and POSTMIX models, together with the HEGADAS/UF_6 model, are used to simulate releases from the open bay doors of the GDP transfer building, where releases may be reactive. Descriptions of the ISCST3 and HEGADAS/UF_6 models can be found in EPA (1995), Post (1994a, 1994b) and Hanna et al. (1995, 1996), and will not be repeated here. The reader is referred to Sect. 4 for a technical description for the models used for the GDP process building release scenario, and Sect. 5 for a technical description for the models used for the GDP transfer building release scenario. This appendix serves as a user's guide for the WAKE, POSTWAKE, UF_6MIXER, and POSTMIX models. Section A.1 describes the I/O structure and input instructions for the models. Section A.2 shows step-by-step instructions as to how to run the models. Section A.3 provides brief descriptions for the models. Guidance to programmers is provided in Sect. A.4.

A.1 INPUT/OUTPUT REQUIREMENTS AND INPUT INSTRUCTIONS

The WAKE model requires one input file (the WKI file, described in detail later), and creates four output files (the WKR, WKO, ISC, and MET files). The WKR file contains a brief summary of the results (other than concentrations) calculated by the WAKE model. The WKO file, which is used as one of the input files to the POSTWAKE model, contains concentration predictions for the part of the plume that is captured in the cavity based on algorithms suggested by Wilson (1995) and Briggs (1996) [i.e., Eqs. (10) and (11)]. Note that because the WKO file is only an intermediate file in the run procedure to be described in Appendix A.2 for the GDP process building scenarios, the user normally does not have to be concerned about that file. The file is automatically generated by WAKE and is automatically read by POSTWAKE. The ISC and MET files contain the input streams and meteorological data, respectively, required to run the ISCST3 model.

The POSTWAKE model requires two input files (the WKO and ISO files) and creates one output file (the OUT file). The WKO file is created by the WAKE model, whereas the ISO file is created by the ISCST3 model. Thus, the user does not have to manually prepare input files for the POSTWAKE model. The OUT file contains the final predicted concentrations at each receptor.

Note that results from many intermediate calculations will be printed by the ISCST3 model because the model is being run in DEBUG mode in order to obtain predicted concentrations at each receptor due to each source. If the scenario involves many sources (e.g., >20) and many receptors (e.g., >50), then the ISO file generated by the ISCST3 model can be large (i.e., many megabytes). The user does not have to be concerned with the details of these large intermediate ISO files produced by ISCST3 because our POSTWAKE model will automatically extract relevant information from the

files, and the final OUT file will be relatively small. The relevant information (steady-state, ground-level concentration; along-wind dispersion coefficient; and cloud advective speed at each receptor associated with each individual source) is summarized in an ".OUX" file.

The UF_6MIXER model requires one input file (the MXI file, described in detail later), and creates four output files (the MXR, MXO, HSI, and LNK files). The MXR file contains a brief summary of the results (other than concentrations) calculated by the UF_6MIXER model. The MXO file, to be used as one of the input files to the POSTMIX model, contains concentrations predicted by the Wilson (1995) and Briggs (1996) models. Note that, like the WKO file, the MXO file is only an intermediate file in the run procedure for the GDP transfer building scenario discussed in Appendix A.2. Thus, the user normally does not have to be concerned about that file. The file is automatically generated by UF_6MIXER, and is automatically read by POSTMIX. The HSI and LNK files are the two input files required to run the HEGADAS/UF_6 model.

The POSTMIX model requires two input files (the MXO and HSR files) and creates one output file (the OUT file). The MXO file is created by the UF_6MIXER model, whereas the HSR file is created by the HEGADAS/UF_6 model. The OUT file contains the final predicted concentrations (from the HEGADAS/UF_6 or Wilson/Briggs model) at each receptor.

All input and output files described above for the WAKE, POSTWAKE, UF_6MIXER, and POSTMIX models are in ASCII format.

The parameters specified in the input (WKI) file for the WAKE model are summarized in the following table. Note that free-format is used and that there should be one parameter specified in each line in the WKI file.

As mentioned in Sect. 4.5, the ISC3 model allows arbitrary lateral distributions for the sources and receptors. However, for the building wake models suggested by Wilson (1995) and Briggs (1996), an implicit assumption is made that all sources and receptors are lined up along the wind direction. Therefore, the lateral offset of the building centerline from the receptor centerline and the distance of the stack from the building centerline are only used by ISC3 and ignored by Eqs. (10) and (11). Figure A.1 shows how various position variables are defined.

Note that, in the following table, parameters related to stack information (e.g., the stack name, the emission rate, the distance between the stack and the downwind edge of the building, etc.) can be repeated up to 100 times. The downwind distance to a receptor can be repeated up to 200 times. That is, the WAKE model can calculate concentrations at up to 200 receptors due to releases from up to 100 sources (the limits on the numbers of receptors and sources are specified by PARAMETER statements in the code and can be easily changed). The model can handle multiple sources simultaneously because releases from the roof vents and stacks on GDP process buildings are treated as passive (inert). Thermodynamics and chemistry calculations are not required for the process building scenario. On the other hand, as shown below, releases from the open bay doors of GDP transfer buildings may be reactive, and thermodynamics and chemistry calculations are required.

Description	Format	Units
Building height	real	m
Building length	real	m
Building width	real	m
Lateral offset of the building centerline from the receptor centerline; > 0, to the right (facing the downwind direction); < 0, to the left of the receptor centerline; see offset in Fig. A.1; only effective for ISC3 calculation	real	m
Stack name (up to 7 characters and no space allowed, the eighth character is reserved by the model; for labeling only)	character	n/a
Pollutant emission rate	real	kg/s
Stack height above the ground	real	m
Stack diameter	real	m
Stack exit velocity (must be > 0 even for a capped stack, in which case the stack exit velocity can be inferred from the requirement of mass conservation)	real	m/s
Stack exit temperature	real	K
Capped indicator (1 = stack is not capped, 2 = stack is capped; use capped option for horizontal-pointing releases)	integer	n/a
Horizontal distance between the stack and the downwind edge of the building	real	m
Lateral distance of the stack from the building centerline; > 0, to the right (facing the downwind direction) of the building centerline; < 0 to the left of the building direction; see Yb in Fig. A.1; only effective for ISC3 calculations	real	m
Release duration (<0 means infinite duration)	real	sec
Repeat the above nine lines for each additional stack		
End-of-stack-input indicator (=ENDS)	character	n/a
Ambient wind speed	real	m/s
Measuring height of ambient wind speed	real	m
Ambient temperature	real	K
Stability indicator (1 = class A, 4 = class D, 6 = class F, etc.)	integer	n/a
Rural/urban indicator (1 = rural, 2 = urban)	integer	n/a
Maximum allowed exposure time (see Sect. 5.4; 1800 seconds recommended)	real	sec
Number of σ_x used to estimate the exposure time (see Sect. 5.4; 2.0 recommended)	real	n/a
Reference exposure time based on which health effects are estimated (3600 seconds recommended)	real	sec
Downwind distance to receptor, as measured from the downwind edge of the building	real	m
Repeat the above line for each additional receptor...		

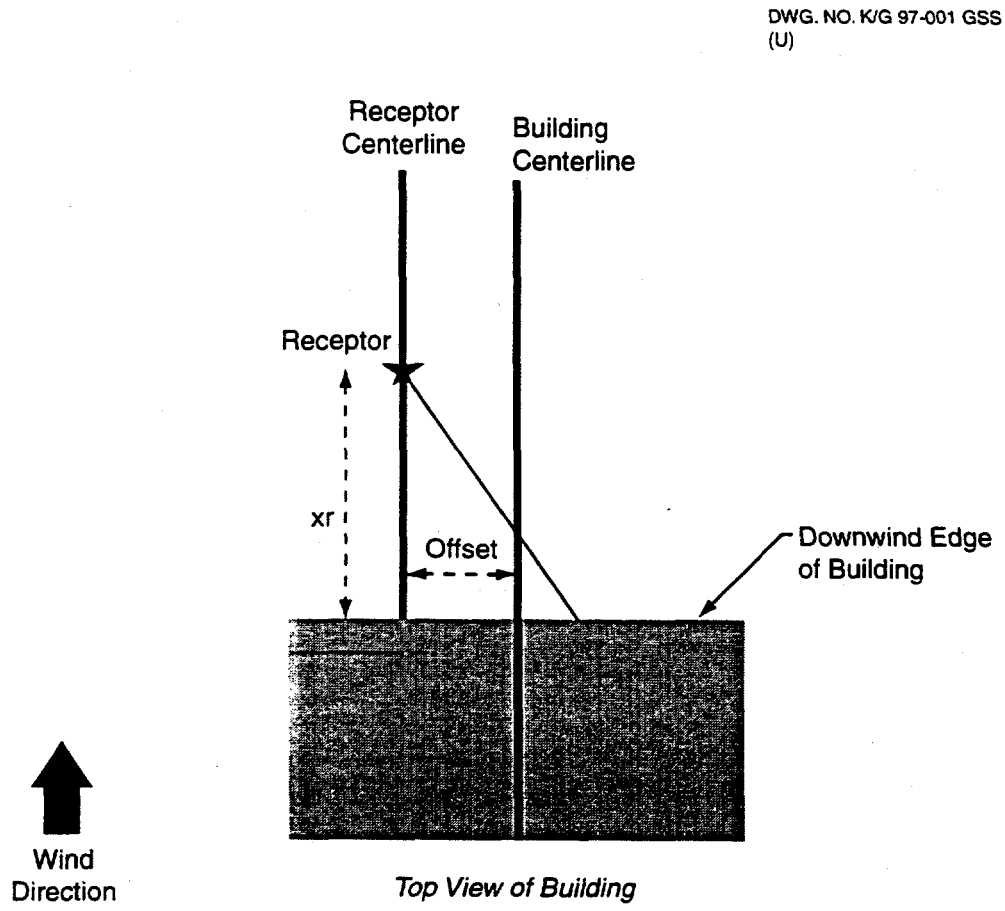

Fig. A.1. Schematic of some inputs required by the WAKE model. Offset: the lateral offset of the building centerline ; xb: the horizontal distance between the stack and the downwind edge of the building; yb: the lateral distance between the stack and the building centerline; and xr: the downwind distance between the receptor and the downwind edge of the building. Offset, xb, yb, and xr are used by the ISC3 model; whereas; only xb and xr are used by the building wake equations [i.e., Eqs. (10) and (11)].

The parameters specified in the input (MXI) file for the UF_6MIXER model are summarized in the following table. Note that free-format is used and that there should be one parameter specified in each line in the MXI file.

Description	Format	Units
Building height	real	m
Building length	real	m
Building width	real	m
Ambient wind speed	real	m/s
Measuring height of ambient wind speed	real	m
Stability indicator (1 = class A, 4 = class D, 6 = class F, etc.)	integer	n/a
Ambient temperature in the building	real	K
Ambient relative humidity (in fractions) in the building	real	n/a
Ambient temperature outside the building	real	K
Ambient relative humidity (in fractions) outside the building	real	n/a
Surface roughness	real	m
Rural/urban indicator (1 = rural, 2 = urban)	integer	n/a
Release duration (<0 means infinite duration)	real	sec
Molecular weight for UF_6	real	kg/kmole
Initial pollutant temperature for stream 1	real	K
Initial plume mass emission rate for stream 1	real	kg/s
Initial mass fraction of air in the plume for stream 1	real	n/a
Initial mass fraction of HF in the plume for stream 1	real	n/a
Initial mass fraction of gaseous UF_6 in the plume for stream 1	real	n/a
Initial mass fraction of liquid UF_6 in the plume for stream 1	real	n/a
Initial mass fraction of total UF_6 in the plume for stream 1	real	n/a
Initial mass fraction of UO_2F_2 in the plume for stream 1	real	n/a
Initial mass fraction of water vapor in the plume for stream 1	real	n/a
Initial pollutant temperature for stream 2	real	K
Initial plume mass emission rate for stream 2	real	kg/s
Fraction of the area of the building side occupied by the plume after initial dilution in the building	real	n/a
Maximum allowed exposure time (see Sect. 5.4; 1800 seconds recommended)	real	sec
Number of σ_x used to estimate the exposure time (see Sect. 5.4; 2.0 recommended)	real	n/a
Reference exposure time based on which health effects are estimated (3600 seconds recommended)	real	sec
Downwind distance, measured from the downwind edge of the building, of receptor	real	m
Repeat the above line for each additional receptor...		

Note that, in the above table, the downwind distance to a receptor can be repeated up to 200 different times. That is, a maximum of 200 receptors can be specified in the UF_6MIXER model (the limit on the number of receptors is specified by a PARAMETER statement in the code and can be easily changed).

Under a special circumstance to be described later, the UF_6MIXER code can model two streams released simultaneously. Two types of releases are allowed for the primary (first) stream, which must be either (1) a pure liquid UF_6 release, or (2) a release of any combination of air, HF, gaseous UF_6, solid UF_6, UO_2F_2 and water vapor (but no liquid UF_6). For the latter type of release, the initial mass fractions of the various components and the initial plume temperature should be as close to a state of thermodynamic equilibrium as possible. Note that the initial mass fractions of air, HF, total UF_6, UO_2F_2 and water vapor for the primary (first) stream must add up to 1.0. If the release for the first stream is pure liquid UF_6, then a second stream, which must be pure gaseous UF_6, can also be included in UF_6MIXER. Note that, in the above table, the two lines of data for the second stream should still be present even for cases where the second stream does not exist. As long as the *total* release consists of multiple phases of UF_6 or multiple components, UF_6MIXER will first perform equilibrium calculations for the plume. If it is found that the plume states specified by the user are not in thermodynamic equilibrium, then the UF_6MIXER model will keep the plume temperature unchanged and readjust the plume composition until an equilibrium is reached. The user is cautioned that it is possible that the UF_6MIXER program may fail to find an equilibrium solution if the specified initial plume states are far from thermodynamic equilibrium.

As described in Sect. 5, for releases from the open bay doors of the GDP transfer building, both the HEGADAS/UF_6 and Wilson/Briggs [i.e., Eqs. (10) and (11)] concentrations. The HEGADAS/UF_6 model is a separate program, whereas the Wilson/Briggs model is implemented in the UF_6MIXER code as a subroutine. The HEGADAS/UF_6 model includes a complete thermodynamics and chemistry treatment for a reactive UF_6 plume. The Wilson/Briggs model, on the other hand, assumes that the plume is well-mixed and not dense. Therefore, the source information required by the Wilson/Briggs model includes the plume mass emission rate and the plume buoyancy flux *after* all chemical reactions have finished, while the source information required by the HEGADAS/UF_6 model includes the plume mass emission rate, the plume temperature, and the plume composition.

The UF_6MIXER model first calculates the initial plume dilution and corresponding chemical reactions that take place in the GDP transfer building. These calculations are made prior to any dispersion calculations in the cavity and at larger distances using the HEGADAS/UF_6 and Wilson/Briggs models, UF_6MIXER accounts for initial plume dilution by treating the building as a "reactor," where the water vapor that is incrementally entrained into the plume is allowed to instantly react with the available UF_6 in the plume (see Sect. 5.1). The plume states after initial dilution are then used to initialize the HEGADAS/UF_6 model at the side of the building. The degree of initial plume dilution is controlled by the user-specified fraction, f_A, of the area of the building side occupied by the plume cross-sectional area. If the user specifies a small f_A, then the plume may be relatively dense and still reactive when it exits the building. If the user specifies a large f_A, then the plume will undergo more dilution before exiting the building. Note that it is possible that the UF_6 in the plume might be completely reacted if the emission rate is small, if f_A

is large, or if the area of the building is large. In this case, the plume coming out of the open bay doors would be inert and may be lighter than air, thus suggesting that there is no need to run the HEGADAS/UF_6 model.

Since the Wilson/Briggs model [i.e., Eqs. (10) and (11)] requires an estimate of the plume buoyancy flux after all chemical reactions have finished (see Sect. 4), the in-building plume dilution modeled by the UF_6MIXER code needs to proceed not only to a point where the plume has grown to the specified size, but also to a point where all chemical reactions are assumed to have taken place so that the final plume buoyancy flux can be estimated. As mentioned above, the point where the plume in the building has grown to the size specified by the user may occur before or after all chemical reactions have completed in the building.

There is no need to specify the concentration averaging time, T_a, in the input file for the UF_6MIXER code. T_a will be set to the exposure time in the code.

The error-function correction as implemented in the HGSYSTEM model (Post, 1994b) and described in Sect. 5.4 is applied to the predicted concentrations if the release duration is finite (i.e., when the release duration specified in the input file is positive). The correction is implemented in both the UF_6MIXER and POSTMIX programs. Note that sometimes it is not necessary to run HEGADAS/UF_6, and thus POSTMIX, if the chemical reactions are completed in the transfer building.

The effects of concentration averaging time, T_a, are assumed to apply to (1) the Gaussian part of Eq. (11) (i.e., the last term in the denominator), and (2) the concentrations (both at the centerline and off the centerline) predicted by the HEGADAS/UF_6 model. It is assumed that the predicted concentration varies with T_a according to $T_a^{-0.2}$ (see Eq. 14). The lower limit of T_a, 18.75 sec, is appropriate for an instantaneous release.

A.2 TUTORIAL—HOW TO RUN A TEST CASE

To simulate non-reactive releases from roof vents and exhaust ducts on the GDP process building, the user is first required to manually create (or edit) the input file, say, TEST.WKI, according to Sect. A.1. After the input file has been created, type

WAKE TEST

to run the WAKE model to calculate concentrations for the fraction of the plume that is captured in the cavity. Then type

ISCST3 TEST.ISC TEST.ISO

to run the ISCST3 model to calculate concentrations for the fraction of the plume that escapes the cavity using the routine EPA method (see Sect. 4). If the test case involves many sources (e.g., >20) and many receptors (e.g., >50), the user should make sure that there are at least a few

megabytes of free space on the computer before running the ISCST3 model because the output file from ISCST3 for the test case can become quite large. Finally, type

POSTWAKE TEST

to merge predicted concentrations from both models. The final results are listed in the file TEST.OUT.

The WAKE model considers releases from the process building scenario to be non-reactive. Therefore, thermodynamics and chemistry calculations are not included, and the concentration of a pollutant is directly proportional to its emission rate.
To simulate releases (probably reactive) from the bay doors of the GDP transfer building, the user is first required to manually create (or edit) the input file, say, TEST.MXI, according to Sect. A.1. After the input file has been created, type

UF6MIXER TEST

to run the UF_6MIXER model to determine the plume states after initial dilution in the building, and to calculate concentrations based on the Wilson/Briggs [i.e., Eqs. (10) and (11)] model. If the plume leaving the GDP transfer building is completely reacted, the final results are listed in TEST.OUT, and there is no need to run the HEGADAS/UF_6 model and the POSTMIX postprocessor. If the plume leaving the building is still reactive, then do the following. Type

HSUF6 TEST

to run the HEGADAS/UF_6 model. Type

POSTMIX TEST

to select appropriate predicted concentrations from either the Wilson/Briggs model or the HEGADAS/UF_6 model (see Sects. 5 and A.3 for more details). The final results are listed in TEST.OUT.

Since releases from the GDP transfer building scenario are probably reactive, requiring thermodynamics and chemistry calculations, the UF_6MIXER, HEGADAS/UF_6, and POSTMIX models are used to predict concentrations for UO_2F_2, HF, U and F. This methodology is different from that used in the GDP process building scenario, where releases were considered passive (inert), and the predicted concentration could be assumed to be linearly proportional to the emission rate. In that case, scaled concentrations (C/Q) need to be predicted for only one pollutant.

A.3 DESCRIPTIONS OF MAJOR TASKS PERFORMED BY PROGRAMS

As mentioned earlier, the WAKE, ISCST3, and POSTWAKE models are used to simulate releases from roof vents and stacks on the GDP process building. The UF_6MIXER, HEGADAS/UF_6, and POSTMIX models are used to simulate releases from the open bay doors of

the GDP transfer building. The reader is referred to Sect. 4 for a technical description of the models used for the GDP process building release scenario, and to Sect. 5 for a technical description of the models used for the GDP transfer building release scenario. Descriptions of the ISCST3 and HEGADAS/UF_6 models can be found in EPA (1995), Post (1994a, 1994b), and Hanna et al. (1995, 1996), and will not be repeated here. Note, however, that the ISCST3 model has been modified so that when the effects of building downwash are considered, concentrations at downwind distances less than three building heights are assumed to be equal to the concentration at a downwind distance of three building heights. (The original ISCST3 model does not perform any calculations at downwind distances less than three building heights when the effects of building downwash are considered.) Furthermore, the HEGADAS/UF_6 model has been modified so that, regardless of the stability class specified by the user for the ambient atmosphere, a B stability class is always assumed by the model in the cavity to account for the observed effects of enhanced dilution in building wakes. This special version of HEGADAS/UF_6 can only be used in conjunction with the UF_6MIXER model.

Brief descriptions of major tasks performed by the WAKE, POSTWAKE, UF_6MIXER, and POSTMIX are given below.

The WAKE model carries out the following tasks:

- determination of the dimensions of the cavity,
- calculation of the plume rise in order to estimate the fraction of the plume that is captured in the cavity,
- calculation of concentrations for the part of the plume captured in the cavity based on the Wilson/Briggs model [i.e, Eqs. (10) and (11)],
- estimation of a correction to concentrations for the part of the plume captured in the cavity due to possible plume lift-off based on the Briggs (1996) model, and
- creation of all necessary input files for the ISCST3 model for the part of the plume that escapes the cavity, as suggested in Sect. 4 of this report.

The POSTWAKE code is used to merge the results from two models: (1) the WAKE model for the part of the plume captured in the cavity, and (2) the ISCST3 model for the part of the plume that escapes the cavity.

The UF_6MIXER model performs the following tasks:

- determination of the dimensions of the cavity,
- estimation of the plume states (e.g., the total plume mass emission rate, the plume composition, the plume temperature, etc.) after the assumed in-building initial dilution and associated chemical reactions,

- estimation of the plume buoyancy flux and the equivalent mass emission rates for UO_2F_2, HF, U, and F when all chemical reactions have been completed (the buoyancy flux and the mass emission rates are required by the Wilson/Briggs model),

- calculation of concentrations based on the Wilson/Briggs model, and

- preparation of the required input data for HEGADAS/UF_6 so that the latter can be initialized at the side of the building.

The POSTMIX model performs the following tasks:

- retrieval of the plume geometry and density information from the HEGADAS/UF_6 predictions in order to estimate the downwind distribution of the plume buoyancy flux, which in turn is used to estimate the correction to concentrations predicted by HEGADAS/UF_6 due to possible plume lift-off based on the Briggs (1996) model,

- selection of the UO_2F_2, HF, U, and F concentrations predicted by the HEGADAS/UF_6 or the Wilson/Briggs model at downwind distances less than the length of the cavity based on which model gives higher predicted concentration for U, and

- selection of the UO_2F_2, HF, U, and F concentrations predicted by the HEGADAS/UF_6 or the Wilson/Briggs model at downwind distances greater than the length of the cavity based on which model gives higher predicted concentration for U at the end of the cavity.

A.4 GUIDE FOR PROGRAMMERS

Because all computer programs, including WAKE, POSTWAKE, UF_6MIXER, and POSTMIX were compiled and linked using the Lahey F77L-EM/32 Fortran compiler, the DOS 640 KB memory allocation limit for executable programs does not apply. It is recommended that the user should have at least a 486DX personal computer with 4 MB of memory and 10 MB of free disk space in order to run the models. The WAKE, POSTWAKE, UF_6MIXER and POSTMIX models are self-contained, i.e., all subroutines are collected into a single program unit.

The programs were written in Fortran 77 with some commonly-used Fortran 90 features, including the DO/ENDDO construct, in-line trailing comments, and symbolic names that are up to 31 characters long. Four Lahey compiler-specific subroutines are used: GETCL, CHARNB, TIMER, and DATE. GETCL retrieves arguments (such as the name of the run) from the command line. CHARNB removes trailing blanks from a character string. TIMER returns hundreds of seconds elapsed since midnight. DATE returns the year, month, and date information. GETCL and CHARNB are used in WAKE, POSTWAKE, UF_6MIXER, and POSTMIX. TIMER and DATE are used in UF_6MIXER. These four subroutines usually have their equivalents on other Fortran compilers. If the user decides to port the programs to other computer platforms, proper translation of the four subroutines is required.

As currently implemented, the WAKE model can handle up to 200 receptors and up to 100 sources at a time. The reason why multiple sources can be simultaneously treated is because releases for the GDP process building scenario are considered passive. The UF_6MIXER model can handle up to 200 receptors but only one source at a time. Since releases for the GDP transfer building scenario may be reactive and full thermodynamics and chemistry calculations are required, only one source is treated at a time. The limit on the number of receptors for WAKE and UF_6MIXER and the limit on the number of sources for WAKE are all specified by Fortran PARAMETER statements in the codes, and can be easily changed.

The WAKE, POSTWAKE, UF_6MIXER, and POSTMIX models were all coded without assuming implicit typing, i.e., the "IMPLICIT NONE" statement appears before all other specification and data statements. This makes the programs less prone to coding errors. If the user decides to make changes to the programs where additional variables are introduced, then those variables must first be declared at the beginning of the programs.

The ISCST3 model (version 95250) included in this package was obtained from EPA's SCRAM electronic bulletin board, with the following three changes:

- Some parameters specified in the include file MAIN1.INC were modified so that less computer memory is required by the model.

- Subroutine PCALC in the CALC1.FOR file was modified so that when the effects of building downwash are considered, predicted concentrations at downwind distances less than three building heights equal the predicted concentration at three building heights.

- Subroutine PRTDAY in the CALC4.FOR file was modified so that an exponential format is used to print out predicted concentrations. The real format used in the original ISCST3 is occasionally saturated for cases with large mass emission rates and short downwind distances.

The revised ISCST3 model was also compiled using the Lahey F77L-EM/32 Fortran compiler with the "D1LAHEY" conditional compilation option chosen.